

1 **Mapping Global Non-Floodplain Wetlands**

2

3 Charles R. Lane<sup>1</sup>, Ellen D’Amico<sup>2</sup>, Jay R. Christensen<sup>3,\*</sup>, Heather E. Golden<sup>3,\*</sup>, Qiusheng Wu<sup>4</sup>, and  
4 Adnan Rajib<sup>5</sup>

5

6 <sup>1</sup> U.S. Environmental Protection Agency, Office of Research and Development, Center for Environmental  
7 Measurement and Modeling, Athens, Georgia, United States of America

8 <sup>2</sup> Pegasus Corporation c/o U.S. Environmental Protection Agency, Office of Research and Development,  
9 Cincinnati, Ohio, United States of America

10 <sup>3</sup> U.S. Environmental Protection Agency, Office of Research and Development, Center for Environmental  
11 Measurement and Modeling, Cincinnati, Ohio, United States of America

12 <sup>4</sup> Department of Geography & Sustainability, University of Tennessee, Knoxville, Tennessee, United  
13 States of America

14 <sup>5</sup> Hydrology and Hydroinformatics Innovation Lab, Department of Civil Engineering, University of Texas  
15 at Arlington, Arlington, Texas, United States of America

16

17 \* These authors contributed equally to this work

18

19 **Correspondence:** Charles Lane (lane.charles@epa.gov) and Ellen D’Amico (damico.ellen@epa.gov)

20

21 **Abstract.** Non-floodplain wetlands – those located outside the floodplains – have emerged as integral  
22 components to watershed resilience, contributing hydrologic and biogeochemical functions affecting  
23 watershed-scale flooding extent, drought magnitude, and water-quality maintenance. However, the  
24 absence of a global dataset of non-floodplain wetlands limits their necessary incorporation into water  
25 quality and quantity management decisions and affects wetland-focused wildlife habitat conservation

26 outcomes. We addressed this critical need by developing a publicly available Global NFW (non-  
27 floodplain wetland) dataset, comprised of a global river-floodplain map at 90 m resolution coupled with a  
28 global ensemble wetland map incorporating multiple wetland-focused data layers. The floodplain,  
29 wetland, and non-floodplain wetland spatial data developed here were successfully validated within 21  
30 large and heterogenous basins across the conterminous United States. We identified nearly 33 million  
31 potential non-floodplain wetlands with an estimated global extent of over 16 million km<sup>2</sup>. Non-floodplain  
32 wetland pixels comprised 53% of globally identified wetland pixels, meaning the majority of the globe's  
33 wetlands likely occur external to river floodplains and coastal habitats. The identified Global NFWs were  
34 typically small (median 0.039 km<sup>2</sup>), with a global median size ranging from 0.018-0.138 km<sup>2</sup>. This novel  
35 geospatial Global NFW static dataset advances wetland conservation and resource-management goals  
36 while providing a foundation for global non-floodplain wetland functional assessments, facilitating non-  
37 floodplain wetland inclusion in hydrological, biogeochemical, and biological model development. The  
38 data are freely available through the United States Environmental Protection Agency's Environmental  
39 Dataset Gateway ([https://gaftp.epa.gov/EPADDataCommons/ORD/Global\\_NonFloodplain\\_Wetlands/](https://gaftp.epa.gov/EPADDataCommons/ORD/Global_NonFloodplain_Wetlands/)) and  
40 through <https://doi.org/10.23719/1528331> (Lane et al., 2023).

41

## 42 **1 Introduction**

43

44 Wetlands are recognized as globally important ecosystems providing functions leading to critical  
45 provisioning (e.g., food, fresh water for domestic, agricultural, and industrial use) and regulating services  
46 (e.g., flood and drought mitigation, water purification and waste treatment, and habitat; Millennium  
47 Ecosystem Assessment, 2005). Despite their functional importance, wetlands are threatened worldwide by  
48 myriad anthropogenic disturbances, including sea-level rise (IPCC, 2014), drainage and filling (Davidson  
49 et al., 2014), water abstraction (Liu et al., 2017), consolidation (McCauley et al., 2015), invasive species  
50 (Zedler and Kercher, 2004), and changing precipitation and temperature patterns (Winter, 2000). These  
51 widespread and globally prevalent alterations to wetlands affect their functioning, resulting in increased

52 downgradient flooding (Golden et al., 2021), modified stream baseflows (Buttle, 2018), reduced pollution  
53 mitigation (Evenson et al., 2018a), and habitat loss (Uden et al., 2015).

54

55 Watershed-scale wetland management is currently hampered by the paucity of accurate and fine-grained  
56 maps of wetland location (Creed et al., 2017; Christensen et al., 2022). However, methods to identify  
57 existing aquatic systems, including wetlands, that provide functions at global scales have recently  
58 emerged, such as the Landsat-based 30 m global surface-water inundation data (Pekel et al., 2016), finer-  
59 resolution satellite-based landcover maps (e.g., Zanaga et al., 2021), and groundwater-driven aquatic  
60 system characterizations (Fan et al., 2013). In addition, methods utilizing digital elevation models to  
61 identify topographic depressions likely to support aquatic systems with characteristic wetland features,  
62 such as saturated soils and/or ponded waters, have also regionally proliferated (Wu et al., 2019a; Wu et  
63 al., 2019b; Christensen et al., 2022).

64

65 These advancements in mapping wetland location, such as those located within the river floodplain or  
66 geographically distal from floodplains, allow resource managers to better incorporate wetland  
67 biogeochemical, hydrological, and biological functions and concomitantly ecosystem services into their  
68 decision-making efforts. For instance, incorporating *floodplain* wetlands into decision-making advances  
69 the wise management and conservation of mapped riparian ecosystems (Tullos, 2018; Kundzewicz et al.,  
70 2018). Thus, recognizing the importance of wetlands located within active river floodplains, land-  
71 management decisions are being made to quantify the functions and ecosystem services of these wetlands  
72 and incorporate them into watershed-scale hydro-ecological decisions (e.g., Makungu and Hughes, 2021;  
73 Rajib et al., 2021).

74

75 However, *non-floodplain wetlands* are typically not incorporated into watershed-scale conservation and  
76 management planning (e.g., Sullivan et al., 2019), thereby ignoring their contributions to watershed-scale  
77 resilience in response to biogeochemical and hydrological disturbances (Rains et al., 2016; Golden et al.,

78 2021; Lane et al., 2022). Non-floodplain wetlands are abundant inland freshwater wetlands located  
79 distally from the floodplains of rivers and lakes (Lane and D'Amico, 2016; Lane et al., 2018). Though  
80 typically small (Cohen et al., 2016), high biogeochemical processing rates within non-floodplain wetlands  
81 have resulted in these systems being termed bioreactors (Marton et al., 2015). Indeed, a literature review  
82 of over 600 articles found that the highest reactivity rates (pollutant mass removal per unit time) were  
83 found in the smallest water bodies and wetlands (Cheng and Basu, 2017). Further, the high reactivity of  
84 individual non-floodplain wetlands can cumulatively improve downgradient water quality conditions  
85 (Golden et al., 2019; Evenson et al., 2021). Non-floodplain wetlands may therefore have an outsized  
86 impact on a watershed's water quality.

87

88 Non-floodplain wetlands are also important ecosystems affecting water quantity (i.e., for storing and  
89 gradually releasing water to downgradient rivers and streams). Specifically, precipitation is captured and  
90 stored in non-floodplain wetlands prior to being discharged downgradient. During this storage period,  
91 water can infiltrate to recharge aquifers, evaporate or transpire, or eventually “spill” overland and be  
92 transported downstream (Jones et al., 2018; Buttle, 2018). These non-floodplain wetland water storage  
93 functions attenuate storm flows (Shaw et al., 2012; Fossey and Rousseau, 2016; Blanchette et al., 2022)  
94 and recharge groundwaters (Bam et al., 2020), thereby mitigating flood-hazards (Mclaughlin et al., 2014)  
95 and ameliorating drought conditions by maintaining baseflow (Ameli and Creed, 2019).

96

97 Despite the important functions provided by non-floodplain wetlands (Biggs et al., 2017; Chen et al.,  
98 2022) a substantive data gap remains: no global maps or datasets exist identifying the geospatial location  
99 of non-floodplain wetlands and open waters. Regionally focused efforts, such as the recent work by Lane  
100 and D'Amico (2016) and Lane et al. (2022) mapped the extent of non-floodplain wetlands (also known as  
101 geographically isolated wetlands, Leibowitz, 2015; Mushet et al., 2015) across the geospatially data-rich  
102 conterminous United States (CONUS, see abbreviation list in Appendix A). They found that 16-23 % of

103 freshwater systems were potential non-floodplain wetlands, suggesting a substantial yet hitherto unknown  
104 portion of the globe's wetlands are likely also this vulnerable water resource.

105  
106 Fortunately, geospatial data for identifying aquatic systems, including wetlands, are burgeoning. Global  
107 land cover and land use geospatial datasets that include a wetland cover class continue to propagate (Hu  
108 et al., 2017a), taking advantage of both lengthy time-series Landsat data (Homer et al., 2020) as well as  
109 recently launched advanced high-resolution and/or synthetic aperture radar (SAR) equipped satellites  
110 (e.g., Sentinel-1, Sentinel-2, plus many commercially available platforms; Martinis et al., 2022) and  
111 topographic data sources and analyses (e.g., Wu et al., 2019b). Examples include the GlobeLand30 (Chen  
112 et al., 2015), the European Space Agency (ESA) WorldCover 2020 (ESA, 2020), the Dynamic World  
113 (Brown et al., 2022), as well as consortiums focusing on annual land cover change mapping (e.g.,  
114 Tsendbazar et al., 2021). Several recent publications review the available wetland-focused datasets,  
115 including Hu et al. (2017a, their Table 1), Davidson et al. (2018, their Table S1), Tootchi et al. (2019,  
116 their Table 1), and Zhang et al. (2023, their Table 1). We summarize additional emerging global land  
117 cover data sets related to surface water and wetlands in Appendix Table B1.

118  
119 Lehner and Döll (2004) were amongst the first to publish a geospatially explicit global map focusing on  
120 wetland extents. Their Global Lakes and Wetlands Database provides 1 km estimates of wetland  
121 abundance. More recent and/or higher resolution wetland-focused datasets have emerged, including the 1  
122 km global dataset from Hu et al. (2017b) that incorporates precipitation and a topographic wetness index,  
123 and the multi-sourced 500 m composite maps of regularly flooded and groundwater-driven wetlands by  
124 Tootchi et al. (2019). Tootchi et al.'s (2019) approach identified small and scattered wetlands. However,  
125 they recognized the limitations inherent in their global product (ca. 500 m per pixel resolution) resulted in  
126 omission errors for many wetland systems, especially those smaller than their 500 x 500 m (25 ha) data  
127 resolution. This suggests, and Tootchi et al. (2019) acknowledged, that many (non-floodplain) wetlands  
128 were omitted in the Tootchi et al. (2019) 500 m global product. Cohen et al. (2016) determined non-

129 floodplain wetlands in the CONUS are “unambiguously small”, e.g., their average non-floodplain wetland  
130 area was just over two hectares (2.1 ha). Based on the “all or nothing” methodological approach in  
131 Tootchi et al. (2019), > 12.5 ha of a given 25.0 ha cell [one homogenous pixel] would have to be  
132 identified as wetland in their resampling of the finer-scale data – much larger than the average 2.1 ha  
133 wetlands found in Cohen et al. (2016).

134  
135 Concurrent with increasingly available global land cover and wetland data, there is an increasing global  
136 focus on deriving floodplain and flood hazard-prone areal extents within river networks based on high-  
137 resolution topographic data coupled with hydrologic and/or hydraulic modeling (Tullos, 2018;  
138 Kundzewicz et al., 2018). The past decade has seen development of multiple regional to continental flood  
139 models that span physically based approaches (e.g., 1-,2-, and 3-D hydrodynamic models) to empirical  
140 models (including machine-learning approaches and statistical models) (see review by Mudashiru et al.  
141 2021). On the global scale, openly accessible global flood models include those reviewed by Hoch and  
142 Trigg (2019), namely CaMa-Flood (Yamazaki et al. 2011), GLOFRIS (Winsemius et al. 2013), JRC  
143 (Dottori et al. 2016), CIMA-UNEP (Rudari et al. 2015), Fathom (Sampson et al. 2015), and ECMWF  
144 (Papperberger et al. 2012). For instance, Sampson et al. (2015) created a global 90 m map of flood-prone  
145 areas between 60° N and 56° S using a regional flood-frequency model. More recently, Nardi et al. (2019)  
146 published a global floodplain dataset at 250 m resolution that extended from 60° N to 60° S developed  
147 through a geomorphic or terrain-based analyses of floodplain elevations and maximum flood-prone areas  
148 using a drainage-area scaling variable (Rajib et al. 2021). The evolution of the MERIT Hydro 90 m global  
149 hydrography dataset by Yamazaki et al. (2019) and machine-learning approaches (e.g., Zhao et al. 2021)  
150 has created additional opportunities to further advance the derivation of global floodplains, with improved  
151 identification of flow accumulation area, river-basin shape, and river channel location.

152  
153 These wetland-location and floodplain-extent data are critical for watershed-scale sustainable aquatic  
154 resource policy decisions (Creed et al., 2017; Golden et al., 2017). The lack of these data can result in

155 disproportionately large model errors and potentially misguided management decisions when non-  
156 floodplain wetlands are not incorporated in hydrological and biogeochemical models, ignoring their  
157 watershed-scale impacts on flooding, drought, and water quality (Evenson et al., 2018a; Rajib et al., 2020;  
158 Golden et al., 2021).

159

160 Here, we provide the first global geospatial dataset of non-floodplain wetlands. We incorporate the recent  
161 development of a high-resolution global floodplain mapping algorithm based on digital terrain models by  
162 Nardi et al. (2019). We couple these spatial floodplain data with higher-resolution modifications to the  
163 gridded global wetland and open water data layers developed by Tootchi et al. (2019) that incorporate the  
164 Pekel et al. (2016) satellite-based inundation product, modeled groundwater-driven wetland extent (Fan et  
165 al. (2013), and ancillary satellite landcover data from Herold et al. (2015). We test the applicability of our  
166 global dataset of non-floodplain wetlands in 21 large and spatial-data rich watersheds spanning nearly  
167 700,000 km<sup>2</sup> across the CONUS. This novel global product identifying non-floodplain wetlands provides  
168 for the quantification and estimation of the locations and extent of important aquatic systems with  
169 abundant hydrological, biogeochemical, and biological functions, filling a noted research gap while  
170 delivering useful data for informed natural resource decision-making and management (Creed et al.,  
171 2017; Lane et al., 2022).

172

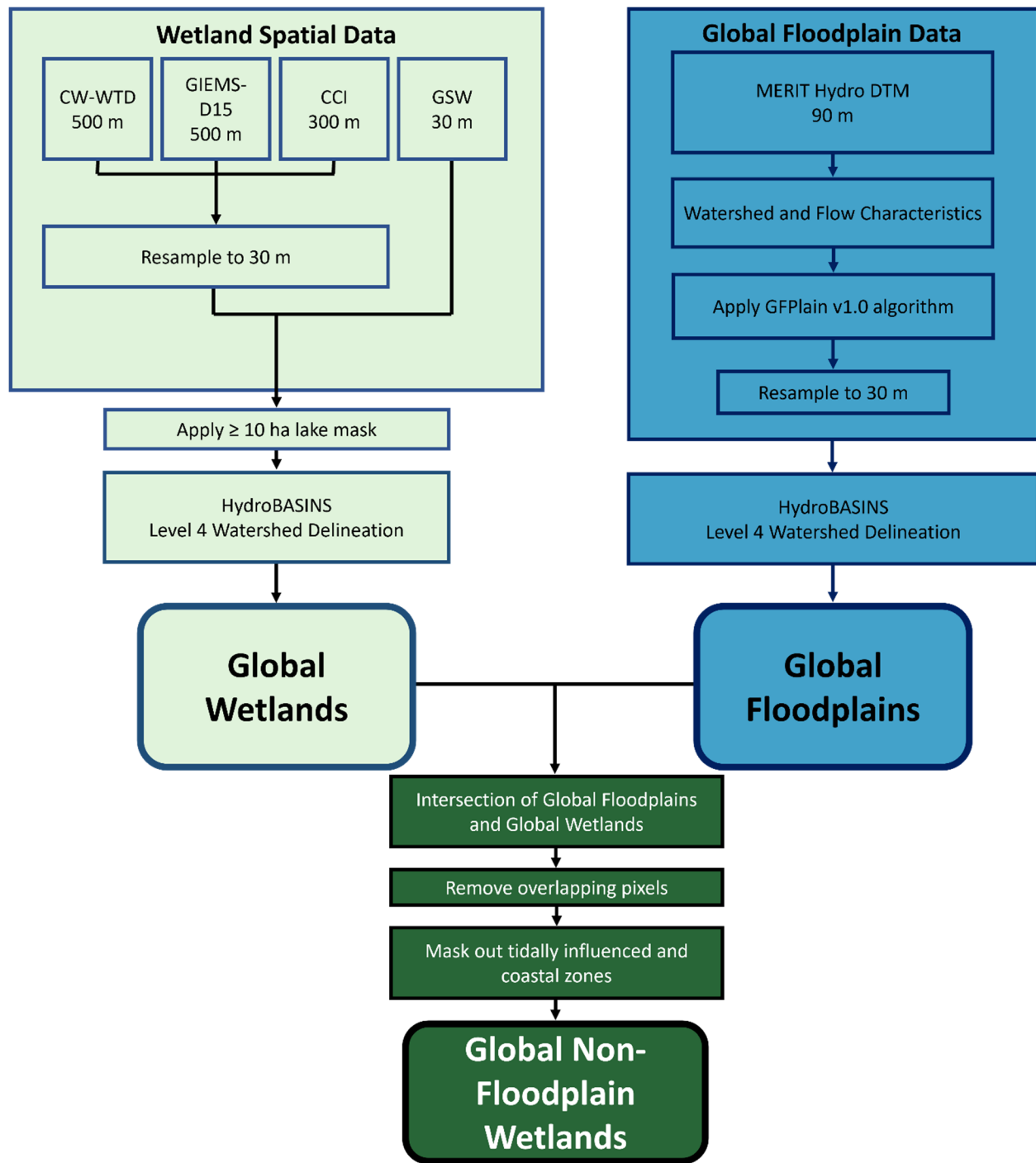
## 173 **2 Methodology and data**

174

175 Identifying global non-floodplain wetlands required the following steps: 1) determination of global  
176 floodplain extent, 2) identification of the global distribution of wetlands, 3) spatial overlay (masking) of  
177 floodplains and wetlands to derive a non-floodplain wetland data layer, and 4) data verification and  
178 accuracy assessment. Steps 1-3 are outlined in a flow chart given in Fig. 1.

179

180



181  
 182 **Figure 1.** Data flow chart identifying the main data sets and processes involved in deriving the Global Floodplain  
 183 and Global Wetland data layers, as well as the intersection of those data to create the Global Non-floodplain  
 184 Wetlands data product. Curved boxes represent final products, and abbreviations may be found in the text and  
 185 Appendix A.



## 186 2.1 Global floodplain data

187

188 Nardi et al. (2019) combined space-borne elevation data and terrain analysis with a novel open-source  
189 algorithm to delineate the geomorphic floodplains across the globe between 60° N and 60° S latitudes.  
190 Conceptually, Nardi et al. (2019) identified floodplains from surrounding hillslopes as those low-lying  
191 landscape features that have been naturally shaped by accumulated geomorphic effects of past flood  
192 events. The original Nardi et al. (2019) dataset was limited in its spatial extent (60° N-60° S) and  
193 resolution (250 m); this study sought to delineate global floodplain extent while concurrently identifying  
194 floodplain features further up the river network than possible with 250 m pixels. Hence, we utilized the  
195 freely available Nardi et al. (2019) GFPlain v1.0 algorithm and coupled this with the MERIT Hydro  
196 (Multi-Error Removed Improved Terrain, Yamazaki et al., 2019), global raster digital terrain model data  
197 to develop a higher resolution (90 m) geomorphic riverine floodplain for the globe, termed hereafter  
198 GFPlain90.

199

200 The development of GFPlain90 required multiple steps. We first extracted elevation data from MERIT  
201 Hydro and reprojected the data in UTM zones to prevent distortion when using the GFPlain algorithm.  
202 We then developed the drainage network, drainage area, flow accumulation and flow direction data from  
203 these data using the established scaling parameters in Nardi et al. (2019; power-law coefficient ( $a$ ) of 0.01  
204 and dimensionless exponent ( $b$ ) = 0.30). We established 20 km<sup>2</sup> as the minimum contributing-area  
205 threshold required to create the drainage network, balancing the development of a global stream-network  
206 distribution and extent with computational requirements. We then globally organized the data by  
207 HydroBASINS Level 4 basins (Lehner and Grill, 2013). HydroBASINS provides seamless watershed  
208 boundaries and subbasin delineations at global scales; there are 1,342 Level 4 HydroBASINS globally.  
209 The floodplain extent resolution of GFPlain90 was resampled (using nearest neighbor) to 30 m for  
210 subsequent performance assessment and overlap analyses with the wetland spatial data. All spatial

211 analyses in this study were conducted using ArcGIS Pro v.2.9.x (ESRI, Redlands, California) and GRASS  
212 GIS v 7.4.4 (OSGEO, Beaverton, Oregon).

213

## 214 **2.2 Global Wetland data**

215

216 Tootchi et al. (2019) developed a widely used composite global wetland map at ~500 m by combining  
217 multiple data sources, including both satellite-based surface-water inundation mapping and vegetation  
218 classification coupled with model-based approaches capturing important groundwater-driven wetland  
219 systems. We specifically used the Tootchi et al. (2019) composite map consisting of both regularly  
220 surface-water flooded wetlands (“regularly flooded wetlands,” RFWs) and groundwater discharge-  
221 maintained wetlands (“groundwater-driven wetlands,” GDWs) as the foundation for our global wetland  
222 map. Tootchi et al. (2019) merged the RFW and GDW maps, described below, to form a union product  
223 used here that demonstrated a high correlation with available evaluation data, called the composite  
224 wetland-water table depth (or CW-WTD).

225

### 226 **2.2.1 Original composite wetland data**

227

228 Regularly flooded wetlands (RFWs) derived by Tootchi et al. (2019) were based on three data sources: 30  
229 m resolution Global Surface Water (GSW) by Pekel et al. (2016), 300 m Climate Change Initiative (CCI)  
230 land cover data by Herold et al. (2015), and 500 m GIEMS-D15 wetland extent data by Fluet-Chouinard  
231 et al. (2015). GSW data used by Tootchi et al. (2019) were developed from Landsat satellite imagery  
232 analyses of pixels identified as inundated at least once during the 32-year period of record by Pekel et al.  
233 (2016). CCI input wetland data for Tootchi et al. (2019) included both inundated and wetland vegetation-  
234 classed pixels assessed during the period 2008-2012 by Herold et al. (2015). For GIEMS-D15, data  
235 included were the mean annual maximum extent of pixels identified as wetlands using multi-sensor  
236 satellite data by Prigent et al. (2007), downscaled to ~500 m resolution by Fluet-Chouinard et al. (2015).

237 GSW and CCI input data were resampled to ~500 m resolution using an “all or nothing” approach by  
238 Tootchi et al. (2019). This means that a pixel categorization of “wetland” at 500 m resolution was given  
239 by Tootchi et al. (2019) only if the majority of resampled finer-resolution input pixels were classed as  
240 wetlands. The upward resampling from 30 m and 300 m to 500 m resulted in a loss of informative spatial  
241 data on wetland extent from GSW and CCI. Tootchi et al. (2019) calculated that RFWs cover  
242 approximately 9.7 % of the global land area (excluding lakes [sourced from (Messenger et al., 2016)],  
243 Antarctica, and the Greenland ice sheet).

244

245 Groundwater-driven wetlands (GDWs in the analysis of Tootchi et al., 2019) used in this study were  
246 based on the water-table depth estimates by Fan et al. (2013). Fan et al. (2013) developed a 1 km  
247 resolution groundwater map based on climate and terrain variables that was validated by over 1 million  
248 government-recorded and published observations. Fan et al. (2013) estimated that shallow groundwater  
249 influenced nearly 15 % of groundwater-fed surface features, explaining important wetland patterning at  
250 global scales (as well as vegetation classes at local and regional scales). A water-table depth threshold of  
251  $\leq 20$  cm was used by Tootchi et al. (2019) to identify groundwater-driven wetlands and they resampled  
252 these data to ~500 m cell resolution. The GDW distribution based on water table depths covered  
253 approximately 15 % of the global land mass (including large portions of the Amazon basin, coastal zones,  
254 and North American and Siberian peatlands).

255

256 Tootchi et al. (2019) created a merged “final” product, called the composite wetland-water table depth  
257 (CW-WTD) map, which is based on the union of the RFW and GDW maps. They measured an  
258 approximately 3.8 % overlap between the total land pixels identified as wetlands in both the RFW and  
259 GDW maps that comprise the CW-WTD, suggesting the different input maps capture different wetland  
260 types. At the global scale, Tootchi et al. (2019) reported spatial Pearson correlations between CW-WTD  
261 (wetland fractions at 3 arcmin, or ~4.9 km grids) and wetlands within GLWD (Lehner and Döll, 2004)

262 and Hu et al. (2017b) as  $r=0.34$  and  $r=0.43$ , respectively. Tootchi et al. (2019, their Table 5 and S1)  
263 provided additional analysis of the correlations between their global wetland product and existing  
264 benchmark data. The total CW-WTD global wetland estimate was  $\sim 21.1\%$  of the land mass, or  
265 approximately 27.5 million  $\text{km}^2$  (excluding large lakes, Antarctica, and the Greenland ice sheet; Tootchi  
266 et al., 2019).

267

## 268 **2.2.2 Derived global wetland data**

269

270 To account for the acknowledged limitations of the Tootchi et al. (2019) data and to accurately identify  
271 more of the existing small and, specifically, non-floodplain wetlands across the globe (e.g., those  $<25$  ha),  
272 we improved upon and augmented the CW-WTD (Tootchi et al., 2019) global wetland data layer with the  
273 30 m native-resolution GSW (Pekel et al., 2016) and 300 m native-resolution CCI (Herold et al., 2015)  
274 data. The inclusive wetland categories of Tootchi et al. (2019) were maintained, namely at least one  
275 inundation event over a 32 year range (for GSW data) and CCI pixels defined as "...mixed classes of  
276 flooded areas with tree covers, shrubs, or herbaceous covers plus inland water bodies..." (Tootchi et al.,  
277 2019, p. 193). However, for our analysis we resampled the 500 m CW-WTD product to 30 m using the  
278 nearest-neighbor approach and then added any identified wetland pixel from the CCI data (resampled  
279 from 300 m to 30 m) and inundated pixel from the GSW data (30 m resolution). Resampling to a finer  
280 resolution (as we did in our analysis) does not result in data losses: the same data are retained but are  
281 divided into equal, smaller parts. However, moving from a finer resolution to coarser resolution (as in the  
282 CW-WTD dataset's "all-or-nothing" approach) does cause data losses: fine-scale data are necessarily  
283 aggregated (often by averaging) to a larger grid cell size, and therefore less information is retained. To  
284 compensate for this data loss in the CW-WTD dataset, the finer resolution GSW (30 m) and CCI (300 m)  
285 data were added back into the dataset. This resulted in a novel and encompassing wetland ensemble end-  
286 product, hereafter termed the Global Wetlands dataset. This new dataset is inclusive of both finer-

287 resolution (30 m and 300 m) data, thereby accounting for a wide range of wetland sizes – such as smaller  
288 non-floodplain wetlands (Cohen et al., 2016) – that remained unmapped by Tootchi et al. (2019).

289

### 290 **2.3 Global Non-Floodplain Wetlands (Global NFWs)**

291

292 To identify non-floodplain wetlands specifically, we overlaid our GFPlain90 floodplain data with our  
293 mapped Global Wetlands data to mask wetland pixels collocated on the floodplain. Then, to avoid tidally  
294 influenced wetlands, we conducted a region-group analysis to identify connected pixels abutting coastal  
295 shorelines in order to mask wetlands in coastal areas (e.g., those directly abutting the shoreline and  
296 spatially connected to tidally influenced areas). We used a four-directional contagion criterion to identify  
297 connected pixels (i.e., those connected in cardinal directions). Subsequently, we applied a 1 km buffer to  
298 the HydroBASINS (Lehner and Grill, 2013) coastline area and removed from our analyses any wetland  
299 region-group partially or completely overlain by the 1 km coastline buffer. In addition, Tootchi et al.  
300 (2019) removed lake systems ( $\geq 10$  ha) from their wetland-focused data by masking aquatic layers using  
301 HydroLAKES (Messenger et al., 2016). To avoid including large lakes in our emerging non-floodplain  
302 wetland geospatial data, we also applied the HydroLAKES mask and removed lake systems  $\geq 10$  ha  
303 (Messenger et al., 2016) from our Global Wetlands dataset. Thus, our final global non-floodplain wetland  
304 data product (hereafter Global NFWs) did not include fluvial floodplain wetlands nor coastal wetland  
305 complexes and large open water lacustrine (lake-like, Cowardin et al., 1979) systems.

306

### 307 **2.4 Data verification and assessment**

308

309 We evaluated the global products developed here through comparison of high-resolution floodplain and  
310 wetland extent data from 21 basins representing disparate climatic (according to the Köppen-Geiger  
311 classification, Beck et al., 2018), elevation, and land-use gradients within the CONUS (Fig. 2;

312 summarized in Table B2). We specifically focused on the CONUS for product assessment because of its  
313 wide-ranging data availability and diversity of physiographic and climatic regions.

314

#### 315 **2.4.1 Verifying floodplain extent**

316

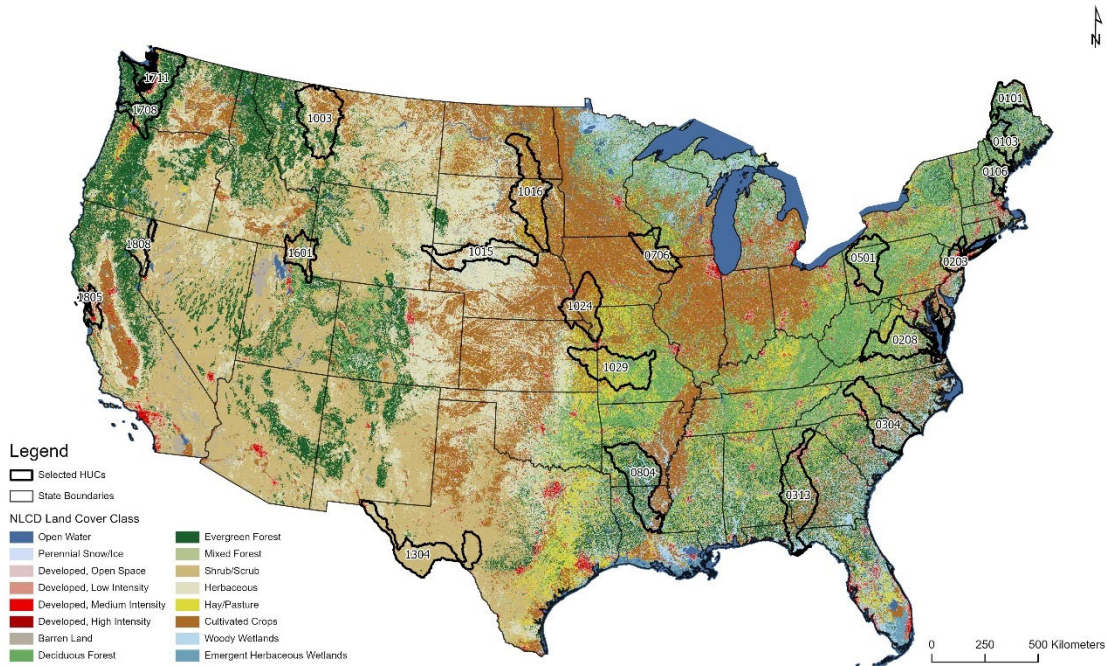
317 We used a recently developed machine learning (ML)-based 30 m resolution CONUS floodplain dataset  
318 (Woznicki et al., 2019) as the benchmark to evaluate our GFPlain90 global floodplain data. Specifically,  
319 the ML model by Woznicki et al. (2019) used the U.S. Federal Emergency Management Agency (FEMA)  
320 100 yr floodplain (i.e., a 1 % chance of coastal or fluvial flood-inundation in a given year; Jakubínský et  
321 al., 2021) as the training data, and subsequently used soil and topographic characteristic along with land  
322 cover to identify potential floodplain grid cells across CONUS at 30 m resolution. Woznicki et al. (2019)  
323 reported that their ML approach correctly identified ~79 % of the FEMA 100 yr coastal and fluvial  
324 floodplains, providing spatially complete 100 yr floodplain coverage totaling 980,450 km<sup>2</sup> across the  
325 CONUS.

326

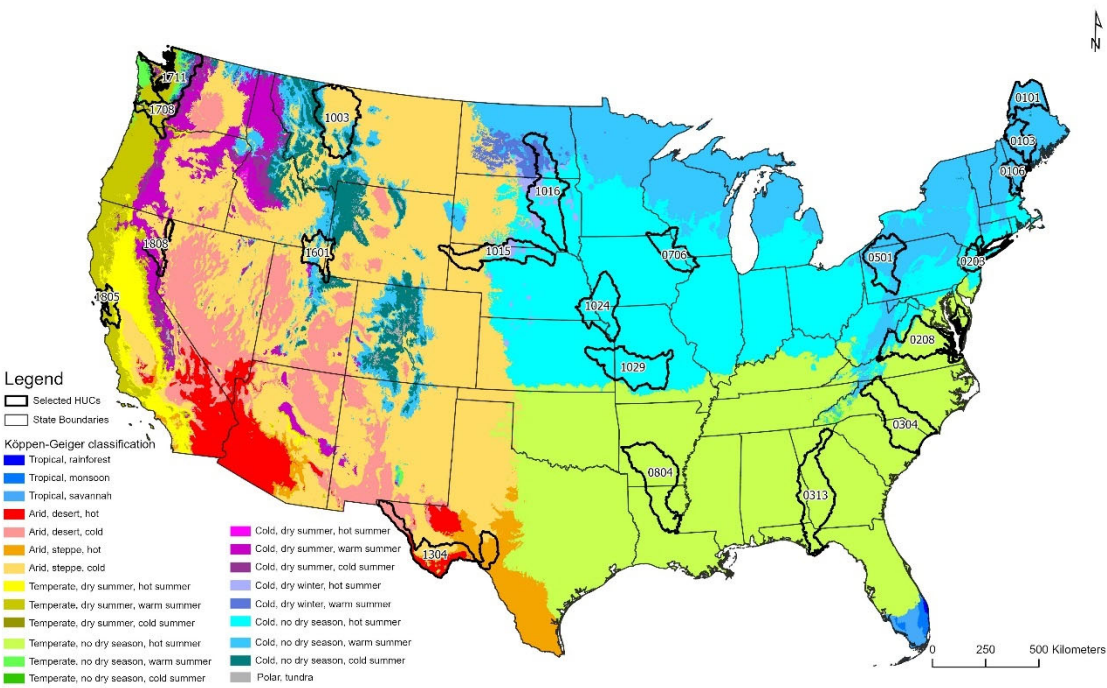
#### 327 **2.4.2 Verifying wetland and non-floodplain wetland extent**

328

329 We evaluated our inclusive Global Wetlands and Global NFWs datasets in 21 basins covering ~680,000  
330 km<sup>2</sup> (Fig. 2). We contrasted our products to the 2016 National Land Cover Database (NLCD, Dewitz,  
331 2019). The NLCD is a 30 m Landsat satellite-based geospatial product with an overall accuracy of 86 %  
332 that incorporates high-resolution aerial imagery of wetland location for model parameterization and  
333 calibration (Jin et al., 2019; Wickham et al., 2021). Three NLCD classes were selected for comparison  
334 with the Global Wetland product: woody wetlands, emergent herbaceous wetlands, and open water. To



335



336

337 **Figure 2.** Twenty-one validation watersheds were selected from across CONUS to capture the breadth and extent of  
 338 land use (top, NLCD 2019) and climate and physiographic regions (bottom) within CONUS according to the  
 339 Köppen-Geiger classification (Beck et al., 2018); also summarized in Table B2). The Hydrologic Unit Code (HUC)  
 340 classifications are sourced from USGS Watershed Boundary Dataset (2022).

341  
 342 assess the relative improvement of our 30 m Global Wetlands and Global NFWs dataset with the 500 m  
 343 Tootchi et al. (2019) data, we also contrasted the CW-WTD with the NLCD classes within the  
 344 verification watersheds. For equal comparisons, following Tootchi et al. (2019) we used the Messenger et  
 345 al. (2016) HydroLAKES to mask out large lake systems ( $\geq 10$  ha) from both the Global Wetlands and the  
 346 NLCD data within the 21 verification watersheds.

347

### 348 **2.4.3 Standard performance measures**

349

350 We evaluated the floodplain and wetland spatial data within the 21 validation watersheds using  
 351 commonly employed performance measures. Following Wing et al. (2017), we first created a contingency  
 352 table for our performance assessment (Table 1). As noted, we selected 20 km<sup>2</sup> as the minimum  
 353 contributing area to develop stream networks in our global floodplain analysis, a reasonable area for flow-  
 354 accumulation that balances computational efficiency for global geospatial model development. Woznicki  
 355 et al. (2019), our benchmark floodplain dataset, used a 4.5 km<sup>2</sup> contributing area in their high-resolution  
 356

357 **Table 1.** Contingency table of possible outcomes for each cell used in assessing the performance of either the  
 358 floodplain or wetland geospatially modeled data. We contrasted published benchmark data from Woznicki et al.  
 359 (2019) for floodplain extent against modeled GFPlain90 data. Wetland comparisons contrasted NLCD wetlands  
 360 (Dewitz, 2019, open water and wetland classes) against both Global Wetlands and Global NFWs data. Table is  
 361 modified from Wing et al. (2017). The subscript “1” equates to a positive outcome or overlapping extent for either  
 362 the modeled (M) or benchmark (B) data whereas a zero means no data overlap or a negative outcome.

	<b>Floodplain [or Wetland] in Benchmark data</b>	<b>Not Floodplain [or Wetland] in Benchmark data</b>
<b>Floodplain [or Wetland] in Modeled data</b>	M <sub>1</sub> B <sub>1</sub>	M <sub>1</sub> B <sub>0</sub>
<b>Not Floodplain [or Wetland] in Modeled data</b>	M <sub>0</sub> B <sub>1</sub>	M <sub>0</sub> B <sub>0</sub>

363



364 CONUS analysis. To appropriately compare between datasets of two varying resolutions, we removed  
365 stream and river network components from the Woznicki et al. (2019) validation dataset developed with  
366 contributing areas  $<20 \text{ km}^2$ , as our model did not discern landscape data at that granularity.

367  
368 To provide a full assessment of our geospatial modeling performance, we contrasted our GFPlain90  
369 floodplain dataset across the 21 validation watersheds using the approaches described below following  
370 Sampson et al. (2015), Wing et al. (2017), and others (e.g., Bates and De Roo, 2000; Alfieri et al., 2014;  
371 Sangwan and Merwade, 2015; Jafarzadegan et al., 2018; Woznicki et al., 2019). We first contrasted our  
372 GFPlain90 floodplains to Woznicki et al. (2019), our benchmark floodplain data. We then analyzed the  
373 watershed-scale comparison of our Global Wetlands product versus the NLCD wetlands (combined open  
374 water and wetland classes), our benchmark wetlands data. We followed with a comparison focusing only  
375 on our Global NFWs data and those NLCD wetlands and open water pixels that were determined to be  
376 non-floodplain systems (i.e., NLCD data that also do not overlap the GFPlain90 data nor coastal waters  
377 and with lakes  $>10 \text{ ha}$  removed). These NLCD wetlands were our benchmark non-floodplain wetland  
378 data. Lastly, we assessed the mean and aggregate error bias of our analyses by exploring results at coarser  
379 spatial granularity (i.e., 1 km pixel size) along the riverine network (for floodplain assessment) and, for  
380 wetland metrics, throughout the entirety of our 21 performance assessment watersheds (Sampson et al.,  
381 2015; Wing et al., 2017). The metrics described below and in Table 2 were used in our analyses.

382  
383 *Hit Rate* (Bates and De Roo, 2000; Horritt and Bates, 2002; Tayefi et al., 2007) also referred to as Recall  
384 (Woznicki et al., 2019) and Correct (Sangwan and Merwade, 2015), measures how well a geospatial  
385 model classification replicates the benchmark data but does not penalize for overprediction. *H* varies from  
386 0, where there is no overlap between the modeled data and the benchmark data, to 1 where the modeled  
387 data completely contain the benchmark data. *Precision* (Woznicki et al., 2019), also known as Spatial  
388 Coincidence (Tootchi et al., 2019), indicates the proportion of the benchmark data that are correctly  
389 predicted and mapped in the modeled data. This metric, *P*, also ranges from 0 to 1 with higher values

390 **Table 2.** Performance metrics used in validation assessments of floodplain and wetland data layers. Data for  
 391 assessment (e.g.,  $M_1B_1$ ) follow that given in Table 1 and modified from Wing et al. (2017), with the exception of  
 392 equations 7 and 8 (see text).

Equation Number	Metrics	Equation	Range
1	Hit Rate (H)	$Hit\ Rate\ (H) = \frac{M_1B_1}{M_1B_1 + M_0B_1}$	0 - 1, higher is “better”
2	Precision (P)	$Precision\ (P) = \frac{M_1B_1}{M_1B_1 + M_1B_0}$	0 - 1, higher is “better”
3	False Alarm Ratio (FA)	$False\ Alarm\ Ratio\ (FA) = \frac{M_1B_0}{M_1B_0 + M_1B_1}$	0 - 1, lower is “better”
4	Critical Success Index (CSI)	$Critical\ Success\ Index\ (CSI) = \frac{M_1B_1}{M_1B_1 + M_0B_1 + M_1B_0}$	0 - 1, higher is “better”
5	F1	$F1 = 2 \left( \frac{H \times P}{H + P} \right)$	0 - 1, higher is “better”
6	Error Bias (EB)	$Error\ Bias\ (EB) = \frac{M_1B_0}{M_0B_1}$	0 - ∞; <1 underprediction, 1 = no bias, >1 indicate overprediction
7	Mean Absolute Error (EA)	$Mean\ Absolute\ Error\ (EA) = \frac{\sum_{i=1}^N  M-B }{N}$	0 - 1, lower is “better”
8	Aggregate Error Bias (BA)	$Aggregate\ Error\ Bias\ (BA) = \frac{\sum_{i=1}^N M-B}{N}$	-1 to 1, negative values indicate underprediction, positive values overprediction

393  
 394 indicating better performance. The *False Alarm Ratio* (Sampson et al., 2015; Wing et al., 2017) also  
 395 known as the False Discovery Ratio, quantifies modeled data overprediction relative to the benchmark  
 396 data. *F* varies from 0 (zero false alarms) to 1 (all false alarms); lower values are considered better  
 397 performance. The False Alarm Ratio can also be calculated as 1 - *Precision* (Woznicki et al., 2019). The  
 398 *Critical Success Index* (CSI, Bates and De Roo, 2000; Aronica et al., 2002; Werner et al., 2005; Fewtrell  
 399 et al., 2008), also known as Jaccard’s Index (Tootchi et al., 2019), and Fit (Sangwan and Merwade, 2015),  
 400 penalizes for both over- and under-prediction, ranging from 0 (no match) to 1 (perfect match). Woznicki  
 401 et al. (2019) utilized a performance metric, *F1*, which combines the *Hit Rate* (called Recall by Woznicki  
 402 et al. 2019) and *Precision* using their harmonic mean. *F1* also varies from 0 to 1, with higher values  
 403 indicating better performance. *Error Bias* (*EB*) characterizes the tendency of the model towards under- or

404 over-prediction (Sampson et al., 2015). Values of 1 indicate no bias,  $0 \leq EB < 1$  indicates underprediction  
405 whereas  $1 < EB \leq \infty$  indicates the model is tending towards overprediction. Lastly, two additional metrics  
406 were calculated that assessed performance at the 30 arc-sec (~1 km) scale. These measures, *Mean*  
407 *Absolute Error* and *Aggregate Error Bias* (Sampson et al., 2015; Wing et al., 2017), characterize the data  
408 accuracy across large spatial extents. Large spatial extents are areas where 30 m data and overlap  
409 accuracy is less a concern than general dataset performance for broad-scale end-user applications (e.g.,  
410 when coarser, watershed-scale “lumped” hydrologic characterizations of water storage are all that is  
411 required). For these metrics, both estimated and benchmark data were resampled to 1 km resolution  
412 across the whole of each watershed; values within each 1 km pixel ranged from 0 to 1 and represented the  
413 fraction of the 30 m resolution estimates and benchmark data. We assessed floodplain estimates after  
414 calculating the fractional abundance comprising each 1 km<sup>2</sup> pixel within a 1 km buffer around the  
415 Woznicki et al. (2019) floodplain data. We additionally analyzed all wetlands at the watershed-scale as  
416 well as focusing on non-floodplain wetlands (e.g., wetlands exclusive of the GFPlain90 floodplain or  
417 coastal connections, our target aquatic system). In Eq. 7 and 8 (given in Table 2),  $M$  is the area estimated  
418 as floodplain (or wetland),  $B$  is the benchmark floodplain (or wetland) area, and  $N$  is the number of 1 km  
419 cells with data. *Mean Absolute Error* and *Aggregate Error Bias* were calculated for each of the 21 HUCs,  
420 following Wing et al. (2017).

421

## 422 **3 Results**

423

### 424 **3.1 Floodplain data performance**

425

426 The GFPlain90 floodplain data (Fig. 3) performed well when contrasted with the 100 yr coastal and  
427 fluvial floodplain extent data from Woznicki et al. (2019), even though our analyses do not map coastal  
428 floodplains. A median Hit Rate of 0.77 suggests that nearly 80% of the benchmark floodplain from  
429 Woznicki et al. (2019) was similarly captured by the GFPlain90 floodplain data (see Appendix Table B3).

430 In addition, the median False Alarm of 0.26 indicates that for every three pixels correctly identified as  
431 within the Woznicki et al. (2019) floodplain, one pixel was incorrectly identified as such (i.e., a  
432 commission error measure); this is evident in wider GFPlain90 floodplains in lower river reaches than  
433 predicted by Woznicki et al. (2019). These performance values are similar to those reported by Woznicki  
434 et al. (2019, False Alarm 0.22) and Wing et al. (2017, False Alarm 0.34-0.37). Critical Success Index  
435 (CSI) scores penalize for over-prediction; our median value of 0.53 approximates previously published  
436 regional (e.g., Sangwan and Merwade, 2015, CSI values ranging from 0.44-0.89) and continental flood-  
437 extent approaches (e.g., Sampson et al., 2015, CSI values from 0.43-0.67; Wing et al., 2017; CSI values  
438 between 0.50 and 0.55 reported). Median Precision (0.74) and F1 (0.70) values approximate those in the  
439 literature as well (e.g., Woznicki et al., 2017 reported values of 0.78 for both). Median Error Bias values  
440 of 1.0 suggests the model neither over-estimates nor under-estimates floodplain extents (Wing et al.  
441 2017). Mean Absolute Error of 0.08 reported here indicates an approximate 8 % difference between our  
442 GFPlain90 model and that of Woznicki et al. (2017) at the 1 km cell resolution.

443

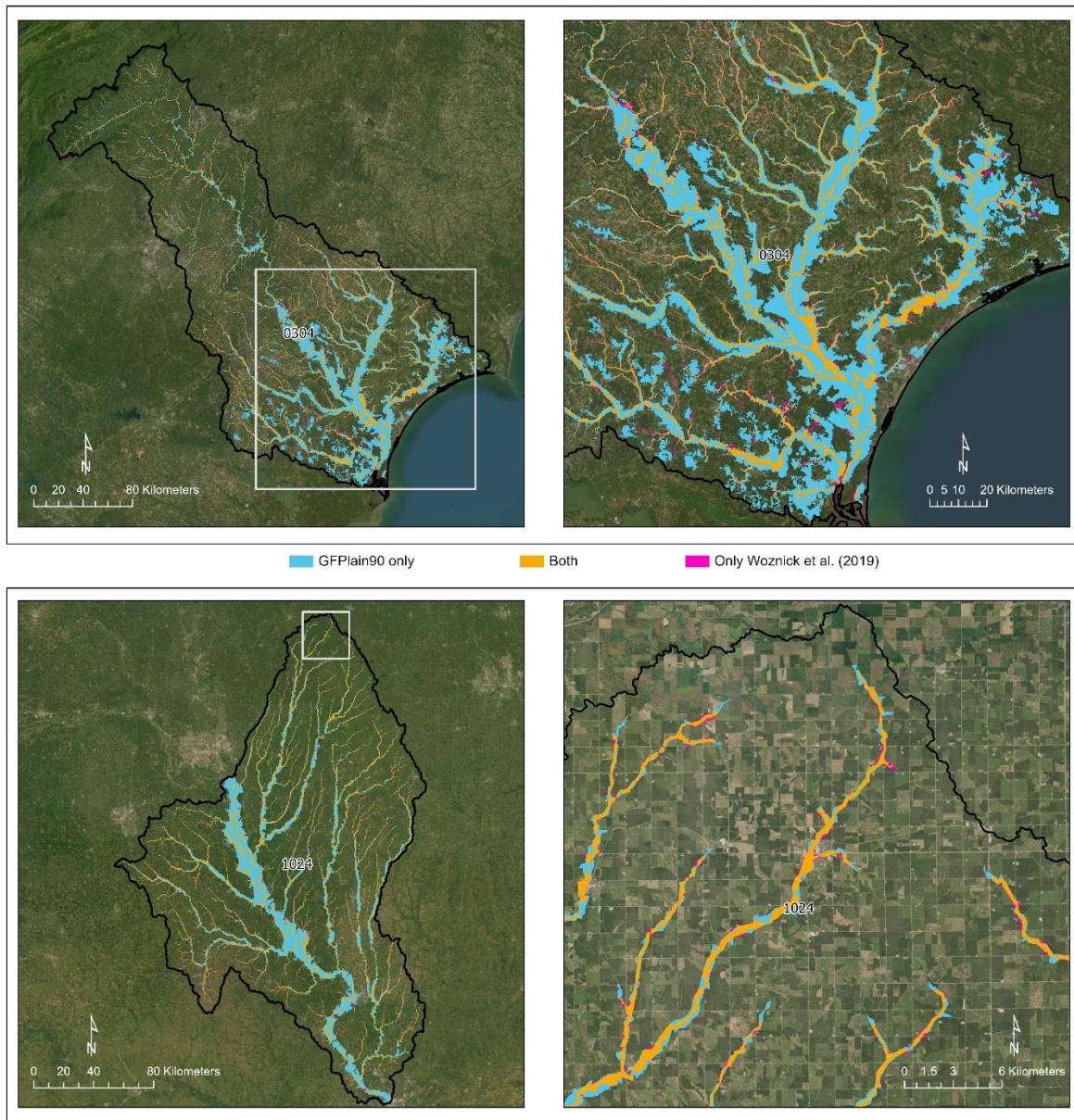
## 444 **3.2 Wetland data performance**

445

### 446 **3.2.1 Global Wetland dataset**

447

448 The novel ensemble Global Wetlands approach improved upon the previously published Tootchi et al.  
449 (2019) research product, the CW-WTD (Table 3) when contrasted with CONUS data. A median Hit Rate  
450 value of 0.24 indicates that both the inclusive Global Wetlands and CW-WTD captured ~one-quarter of  
451 the high-resolution, 30-m pixel size NLCD wetlands and open waters in the validation dataset. However,  
452 across the 21 validation watersheds the Global Wetlands dataset developed here correctly identified more  
453 wetlands than the CW-WTD alone, as indicated by an 8% mean increase in Precision, 43 % increase in  
454 Critical Success Index, 38 % increase in F1, a -8 % decrease in the False Alarm ratio, and a 21 %



456

457 **Figure 3.** The robust performance of GFPlain90 relative to the benchmark Woznicki et al. (2019) floodplain data is  
 458 evident in the two rows, with the top panels (HUC\_0304) a coastal watershed spanning North and South Carolina,  
 459 USA, and the bottom two panels different spatial extents of a midwestern USA watershed (HUC\_1024). The  
 460 mainstem of the river network appeared wider in the GFPlain90 data in both examples, especially in the lower  
 461 reaches, though the complete network was well represented (i.e., floodplains were identified to the furthest extent of  
 462 the stream network's headwaters). Satellite imagery is sourced from ESRI (2022).

463 decrease in Error Bias. At coarser, 1 km<sup>2</sup> scales, there was a slight decrease in the Mean Absolute Error  
464 associated with the Global Wetlands, and no difference in Aggregate Error Bias between the data  
465 products.

466

### 467 **3.2.2 Global Non-Floodplain Wetland (Global NFW) dataset**

468

469 Non-floodplain wetland identification using the Global Wetlands data (i.e., Global NFWs) similarly  
470 improved upon the CW-WTD product (Fig. 4). For instance, though the Hit Rate values were low (e.g.,  
471 median values  $\leq 0.10$ ), underscoring both the difficulty in mapping non-floodplain wetlands and the  
472 challenge of assessing performance using high-resolution data, Global NFW analyses correctly identified  
473 50 % more non-floodplain wetlands than the CW-WTD (Table 4, Tootchi et al., 2019). Improvements  
474 when focusing on non-floodplain wetlands were found in every category with the Global NFWs dataset,  
475 demonstrating increased non-floodplain wetland accuracy versus the original CW-WTD across the  
476 median metric values for Precision, Critical Success Index, F1, False Alarms, and Error Bias (e.g., 33 %  
477 increase in Precision, 20 % increase in Critical Success Index, 10 % increase in F1 scores, and a 12 %  
478 decrease in False Alarms and a 19 % decrease in Error Bias). There was no difference between the  
479 datasets with median values for Mean Absolute Error (median values for both = 0.09) or Aggregate Error  
480 Bias (median values for both = 0.07). Thus, at the 1 km<sup>2</sup> cell size, there was <10 % difference between  
481 both the CW-WTD and the Global NFWs and the benchmark NLCD non-floodplain wetlands and open  
482 waters (with the difference mostly stemming from an increase in identified wetlands with both CW-WTD  
483 and Global NFWs, as indicated with the positive Aggregate Error Bias values).

484

485

486

487

488 **Table 3.** Spatial performance assessment of both the Global Wetland (abbreviated here as GW) and CW-WTD  
489 (abbreviated here as WTD, Tootchi et al., 2019) datasets when contrasted with the benchmark NLCD wetlands  
490 (Dewitz, 2019). The first six equations directly assess the spatial concordance and overlap between each spatial  
491 dataset and the benchmark (e.g., CW-WTD contrasted with the NLCD), whereas Mean Absolute Error (MAE, Eq.  
492 7) and Aggregate Error Bias (AEB, Eq. 8) are coarser fractional analyses measured throughout each watershed (e.g.,  
493 the proportional abundance NLCD within each 1 km<sup>2</sup> cell is contrasted with the proportional abundance of Global  
494 Wetlands predicted correctly within that cell).

Hydrologic Unit Code (HUC) ID	Hit Rate		Precision		False Alarm		Critical Success	
	(Eq. 1)		(Eq. 2)		(Eq. 3)		(Eq. 4)	
	WTD	GW	WTD	GW	WTD	GW	WTD	GW
HUC_0101	0.31	0.32	0.51	0.53	0.49	0.47	0.24	0.25
HUC_0103	0.26	0.28	0.42	0.45	0.58	0.55	0.19	0.21
HUC_0106	0.25	0.27	0.41	0.44	0.59	0.56	0.18	0.20
HUC_0203	0.12	0.12	0.51	0.53	0.49	0.47	0.11	0.11
HUC_0208	0.31	0.33	0.56	0.65	0.44	0.35	0.25	0.28
HUC_0304	0.42	0.43	0.65	0.69	0.35	0.31	0.35	0.36
HUC_0313	0.39	0.41	0.58	0.64	0.42	0.36	0.30	0.33
HUC_0501	0.15	0.17	0.57	0.64	0.43	0.36	0.14	0.15
HUC_0706	0.24	0.25	0.86	0.92	0.14	0.08	0.23	0.24
HUC_0804	0.45	0.46	0.70	0.75	0.30	0.25	0.38	0.40
HUC_1003	0.14	0.16	0.32	0.41	0.68	0.59	0.11	0.13
HUC_1015	0.25	0.40	0.17	0.42	0.83	0.58	0.12	0.26
HUC_1016	0.13	0.16	0.54	0.70	0.46	0.30	0.12	0.15
HUC_1024	0.10	0.10	0.67	0.75	0.33	0.25	0.09	0.10
HUC_1029	0.10	0.13	0.51	0.72	0.49	0.28	0.09	0.13
HUC_1304	0.02	0.02	0.44	0.52	0.56	0.48	0.02	0.02
HUC_1601	0.29	0.33	0.34	0.45	0.66	0.55	0.19	0.24
HUC_1708	0.24	0.24	0.48	0.49	0.52	0.51	0.19	0.20
HUC_1711	0.09	0.10	0.46	0.51	0.54	0.49	0.08	0.09
HUC_1805	0.14	0.15	0.62	0.64	0.38	0.36	0.13	0.13
HUC_1808	0.12	0.13	0.51	0.55	0.49	0.45	0.11	0.11
<b>Median</b>	0.24	0.24	0.51	0.55	0.49	0.45	0.14	0.20
<b>Difference</b>		0.00		0.04		-0.04		0.06
<b>Change (%)</b>		0.0		7.8		-8.2		42.9

495

496 **Table 3.** (Continued)

Hydrologic Unit Code (HUC) ID	F1		Error Bias		MAE		AEB	
	(Eq. 5)		(Eq. 6)		(Eq. 7)		(Eq. 8)	
	WTD	GW	WTD	GW	WTD	GW	WTD	GW
HUC_0101	0.38	0.40	0.43	0.40	0.18	0.17	0.09	0.09
HUC_0103	0.32	0.34	0.50	0.47	0.16	0.15	0.06	0.07
HUC_0106	0.31	0.33	0.49	0.46	0.20	0.19	0.08	0.08
HUC_0203	0.19	0.20	0.13	0.13	0.36	0.36	0.28	0.28
HUC_0208	0.40	0.44	0.35	0.27	0.17	0.17	0.09	0.10
HUC_0304	0.51	0.53	0.39	0.34	0.21	0.21	0.12	0.13
HUC_0313	0.47	0.50	0.48	0.38	0.16	0.16	0.07	0.09
HUC_0501	0.24	0.26	0.14	0.11	0.10	0.10	0.09	0.09
HUC_0706	0.37	0.39	0.05	0.03	0.12	0.12	0.11	0.12
HUC_0804	0.55	0.57	0.36	0.29	0.20	0.20	0.12	0.14
HUC_1003	0.19	0.23	0.34	0.27	0.04	0.04	0.02	0.02
HUC_1015	0.21	0.41	1.59	0.91	0.05	0.04	-0.01	0.00
HUC_1016	0.21	0.26	0.13	0.08	0.26	0.26	0.23	0.24
HUC_1024	0.17	0.18	0.05	0.04	0.14	0.14	0.13	0.14
HUC_1029	0.17	0.22	0.11	0.06	0.11	0.12	0.10	0.11
HUC_1304	0.04	0.04	0.02	0.02	0.08	0.08	0.08	0.08
HUC_1601	0.31	0.38	0.80	0.59	0.05	0.05	0.01	0.01
HUC_1708	0.32	0.33	0.34	0.33	0.15	0.15	0.08	0.08
HUC_1711	0.15	0.17	0.12	0.11	0.17	0.17	0.14	0.15
HUC_1805	0.23	0.24	0.10	0.10	0.25	0.26	0.21	0.21
HUC_1808	0.20	0.20	0.13	0.12	0.09	0.09	0.07	0.07
<b>Median</b>	0.24	0.33	0.34	0.27	0.16	0.15	0.09	0.09
<b>Difference</b>		0.09		0.07		-0.01		0.00
<b>Change (%)</b>		37.5		-20.6		-6.3		0.0

497

498



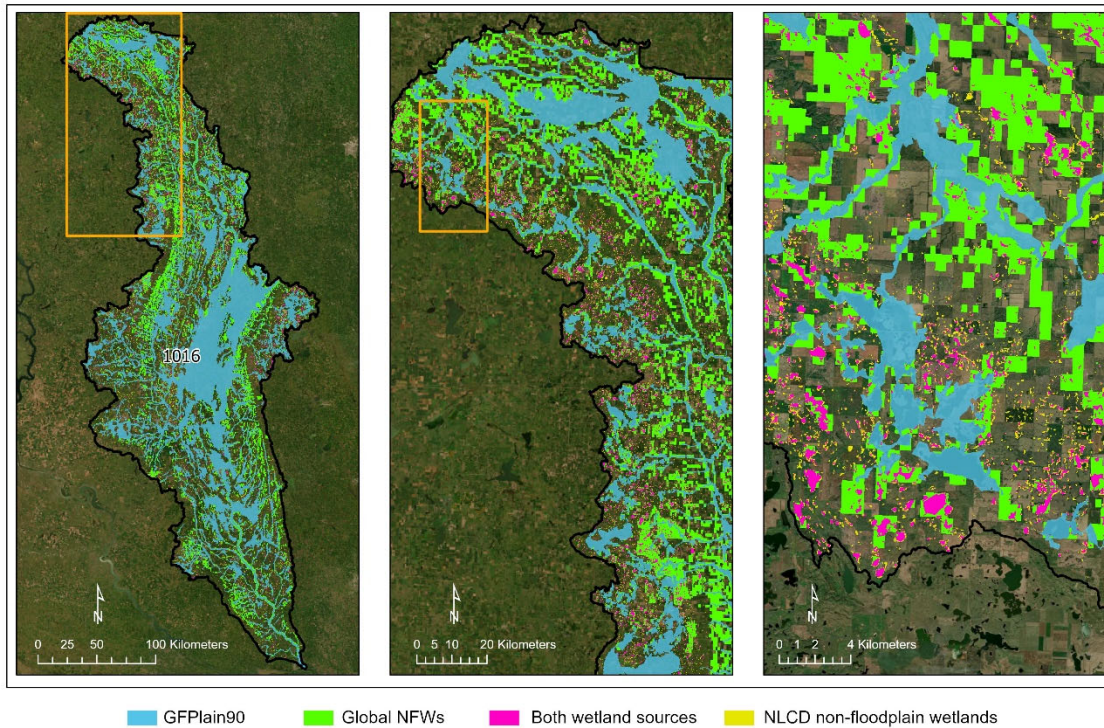


**Figure 4.** Demonstration of the relative accuracy of the Global NFWs in identifying non-floodplain wetlands using a Prairie Pothole Region watershed (HUC\_1016, see Fig. 2) replete with abundant non-floodplain wetlands. Correctly identified wetlands occur in both wetland sources (magenta color). Omission errors (NLCD non-floodplain wetlands, smaller systems in yellow) and commission errors (Global NFWs, green) are evident as a result of the higher resolution of the NLCD validation dataset. Satellite imagery sourced from ESRI (2022). Note the scale increasing from left panel to right panel (i.e., the orange box in the first panel is shown in the second panel at a higher resolution, and the box in the second panel is shown in the last panel at an even higher resolution).

507 **Table 4.** Non-floodplain wetland performance metrics contrasting both the Global NFWs (abbreviated here as  
508 GNFW) and CW-WTD (abbreviated here as WTD, Tootchi et al., 2019) non-floodplain wetland spatial data with the  
509 benchmark NLCD wetlands (Dewitz, 2019). Descriptions of the metrics are the same as in Table 3, though the focus  
510 here is on wetlands outside the GFPlain90-derived floodplain.

Hydrologic Unit Code (HUC) ID	Hit Rate		Precision		False Alarm		Critical Success Index	
	(Eq. 1)		(Eq. 2)		(Eq. 3)		(Eq. 4)	
	WTD	GNFW	WTD	GNFW	WTD	GNFW	WTD	GNFW
HUC_0101	0.24	0.25	0.43	0.45	0.57	0.55	0.18	0.19
HUC_0103	0.17	0.18	0.30	0.32	0.70	0.68	0.12	0.13
HUC_0106	0.15	0.18	0.14	0.17	0.86	0.83	0.08	0.10
HUC_0203	0.12	0.13	0.20	0.23	0.80	0.77	0.08	0.09
HUC_0208	0.14	0.16	0.34	0.41	0.66	0.59	0.11	0.13
HUC_0304	0.26	0.28	0.45	0.49	0.55	0.51	0.20	0.21
HUC_0313	0.21	0.23	0.35	0.40	0.65	0.60	0.15	0.17
HUC_0501	0.05	0.07	0.32	0.41	0.68	0.59	0.05	0.06
HUC_0706	0.05	0.06	0.63	0.72	0.37	0.28	0.05	0.05
HUC_0804	0.30	0.31	0.51	0.55	0.49	0.45	0.23	0.25
HUC_1003	0.04	0.07	0.13	0.21	0.87	0.79	0.03	0.05
HUC_1015	0.07	0.25	0.05	0.28	0.95	0.72	0.03	0.15
HUC_1016	0.07	0.11	0.31	0.53	0.69	0.47	0.06	0.10
HUC_1024	0.02	0.04	0.18	0.41	0.82	0.59	0.02	0.04
HUC_1029	0.03	0.06	0.25	0.58	0.75	0.42	0.03	0.06
HUC_1304	0.00	0.00	0.26	0.33	0.74	0.67	0.00	0.00
HUC_1601	0.05	0.09	0.07	0.16	0.93	0.84	0.03	0.06
HUC_1708	0.06	0.06	0.33	0.35	0.67	0.65	0.05	0.05
HUC_1711	0.04	0.05	0.22	0.27	0.78	0.73	0.04	0.05
HUC_1805	0.06	0.07	0.27	0.30	0.73	0.70	0.05	0.06
HUC_1808	0.05	0.06	0.25	0.36	0.75	0.64	0.04	0.06
<b>Median</b>	0.06	0.09	0.27	0.36	0.73	0.64	0.05	0.06
<b>Difference</b>		0.03		0.09		-0.09		0.01
<b>Change (%)</b>		50.0		33.3		-12.3		20.0

511

512

513 **Table 4.** (Continued)

Hydrologic Unit Code (HUC) ID	F1		Error Bias		Mean Absolute Error		Aggregate Error Bias	
	(Eq. 5)		(Eq. 6)		(Eq. 7)		(Eq. 8)	
	WTD	GFW	WTD	GFW	WTD	GFW	WTD	GFW
HUC_0101	0.31	0.32	0.41	0.39	0.16	0.16	0.08	0.09
HUC_0103	0.21	0.23	0.48	0.46	0.14	0.14	0.06	0.06
HUC_0106	0.14	0.18	1.11	1.03	0.11	0.11	-0.01	0.00
HUC_0203	0.15	0.17	0.53	0.51	0.09	0.09	0.03	0.03
HUC_0208	0.20	0.23	0.32	0.28	0.10	0.10	0.07	0.07
HUC_0304	0.33	0.35	0.44	0.40	0.17	0.17	0.08	0.09
HUC_0313	0.27	0.29	0.51	0.45	0.12	0.12	0.05	0.06
HUC_0501	0.09	0.11	0.12	0.10	0.09	0.09	0.07	0.08
HUC_0706	0.09	0.10	0.03	0.02	0.09	0.09	0.09	0.09
HUC_0804	0.38	0.40	0.43	0.37	0.13	0.13	0.07	0.07
HUC_1003	0.07	0.10	0.32	0.26	0.02	0.03	0.01	0.01
HUC_1015	0.06	0.26	1.46	0.85	0.03	0.02	-0.01	0.00
HUC_1016	0.11	0.19	0.17	0.11	0.15	0.15	0.12	0.13
HUC_1024	0.03	0.07	0.09	0.06	0.05	0.05	0.04	0.05
HUC_1029	0.05	0.11	0.09	0.05	0.08	0.08	0.07	0.07
HUC_1304	0.00	0.01	0.01	0.01	0.06	0.06	0.05	0.06
HUC_1601	0.05	0.11	0.68	0.50	0.02	0.02	0.00	0.01
HUC_1708	0.10	0.10	0.12	0.12	0.11	0.11	0.09	0.10
HUC_1711	0.07	0.09	0.16	0.15	0.09	0.09	0.07	0.07
HUC_1805	0.10	0.11	0.18	0.17	0.10	0.10	0.07	0.07
HUC_1808	0.08	0.11	0.15	0.12	0.02	0.02	0.01	0.01
<b>Median</b>	0.10	0.11	0.32	0.26	0.09	0.09	0.07	0.07
<b>Difference</b>		0.01		-0.06		0.00		0.00
<b>Change (%)</b>		10.0		-18.8		0.0		0.0

514

515

516 **3.3 Global extent analyses and synthesis**

517

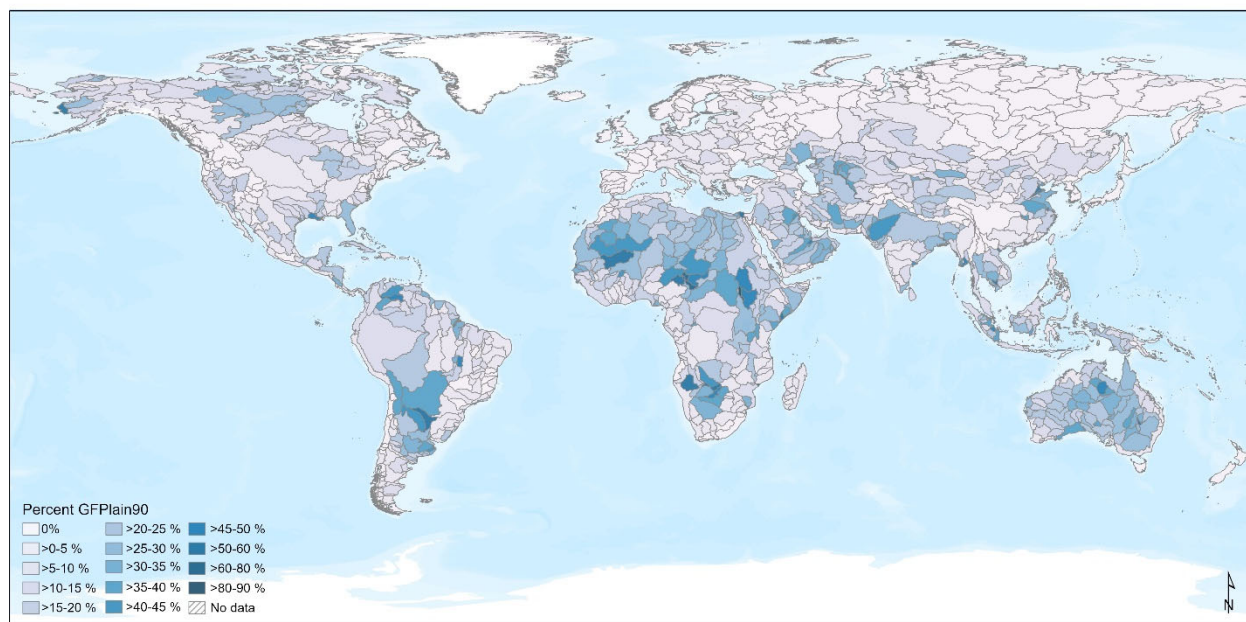
518 **3.3.1 Floodplains**

519

520 Floodplains were estimated to cover 26.6 million km<sup>2</sup> (Table 5), or 19.7 % of the global landmass.

521 Approximately 23-24 % of the African and Australasian land masses were categorized as occurring

522 within a floodplain, the greatest percentage of global areas so categorized. Conversely, the Arctic  
523 (northern Canada and Alaska) and Greenland (excluding the ice sheet) had the least land mass categorized  
524 as floodplain (13-14 %). In comparison, Nardi et al. (2019) calculated a global floodplain extent of  
525 13,394,139 km<sup>2</sup>, using a 250-m pixel size, a 1000 km<sup>2</sup> minimum contributing area, and bounding their  
526 study between 60° N and 60° S latitudes. Our analyses using the same latitudinal bounds but with a higher  
527 resolution dataset (90 m) and a 20 km<sup>2</sup> minimum contributing area identified 24,185,775 km<sup>2</sup>, an 81 %  
528 areal increase (Fig. B1). The relative percent composition of each HydroBASIN that is comprised of  
529 GFPlain90 floodplains is given in Fig. 5.  
530



531  
532 **Figure 5.** Floodplain extents derived from GFPlain90 as a proportion of each of the Level 4 HydroBASINS  
533 (Lehrner and Grill, 2013). The data range demonstrated that up to ~90 % of a given watershed was comprised of  
534 floodplain area, as evidenced by HydroBASINS in south central Africa and central South America. The basemap  
535 layer is the ESRI World Terrain Base (2022).

536  
537

538 **Table 5.** Calculated floodplain area for each HydroBASINS at the global scale. Our analyses found 19.7 % of the  
 539 landmass occurs within a floodplain.

<b>HydroBASINS Region</b>	<b>Floodplain (km<sup>2</sup>)</b>	<b>Floodplain Percent of Landmass</b>
Africa	6,990,859	23.3 %
Arctic (northern Canada & Alaska)	894,594	14.2 %
Asia	4,283,991	20.6 %
Australasia	2,649,395	23.8 %
Europe and Middle East	3,415,308	19.1 %
Greenland (excl. ice sheet)	270,813	12.6 %
North & Central America (excl. Alaska)	2,713,346	17.0 %
Siberian Russia	2,051,305	15.8 %
South America	3,368,778	18.9 %
<b>Total</b>	<b>26,638,389</b>	<b>19.7 %</b>

540

### 541 3.3.2 Wetlands

542

543 Global Wetland extent covered 30.5 million km<sup>2</sup> (Table 6). With a focus on smaller systems compared to  
 544 those presented by Tootchi et al. (2019), our Global Wetland dataset identified 11% more potential global  
 545 wetlands (3 million km<sup>2</sup> additional wetlands). Australasia had the greatest proportional wetland  
 546 abundance (see also Zhu et al., 2022), with wetlands covering 38 % of the landmass (driven, in part, by  
 547 island abundance and fringing estuarine wetlands [Fan et al., 2013]). Greenland (3 %) and Africa (12 %)   
 548 had the least wetlands identified on the land mass.

549

550 **Table 6.** Estimated Global Wetlands areal extent for each of the nine regional HydroBASINS (Lehner and Grill,  
 551 2013). As described in the text, Global Wetlands extent incorporates the CW-WTD (Tootchi et al., 2019), CCI  
 552 (Herold et al., 2015), and GSW (Pekel et al., 2016); lakes of  $\geq 10$  ha have been removed (Messenger et al., 2016).

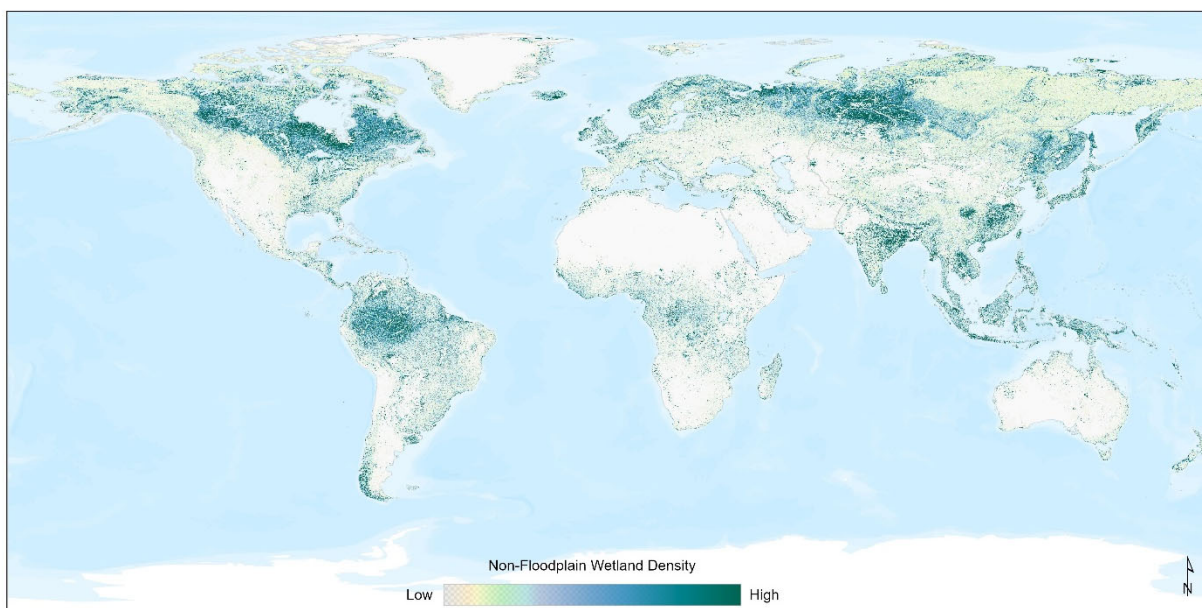
<b>HydroBASINS Region</b>	<b>Wetlands (km<sup>2</sup>)</b>	<b>Wetland Percent of Landmass</b>
Africa	3,524,917	11.8 %
Arctic (northern Canada & Alaska)	1,807,830	28.6 %
Asia	5,543,333	26.6 %
Australasia	4,283,996	38.4 %
Europe and Middle East	2,465,074	13.8 %
Greenland (excl. ice sheet)	60,761	2.8 %
North & Central America (excl. Alaska)	4,107,333	25.8 %
Siberian Russia	3,578,868	27.6 %
South America	5,140,139	28.8 %
<b>Total</b>	<b>30,512,251</b>	<b>22.6 %</b>

### 553 3.3.3 Non-floodplain wetlands (Global NFW)

554

555 Approximately 16.0 million km<sup>2</sup> of potential non-floodplain wetlands were identified globally (Global  
556 NFWs, Fig. 6), meaning that 11.9 % of the global landmass is estimated to be covered by non-floodplain  
557 wetlands (Table 7). This represents ~53 % of the total global wetlands found in the dataset used in this  
558 analysis (see Methods: Wetland Data, above). The global distribution of non-floodplain wetlands is  
559 widespread, though they were found to comprise a higher proportion of wetlands within more northern  
560 HydroBASINS watersheds (i.e., higher abundances in formerly glaciated basins), as demonstrated in Fig.  
561 7. The Arctic portion of northern Canada and Alaska (21.7 %), and Siberian Russia (17.4 %), typically  
562 underlain by permafrost and frequently inundated or saturated due to poor drainage evolution  
563 (Kremenetski et al., 2003; Robarts et al., 2013; Olefeldt et al., 2021), had the greatest percent non-

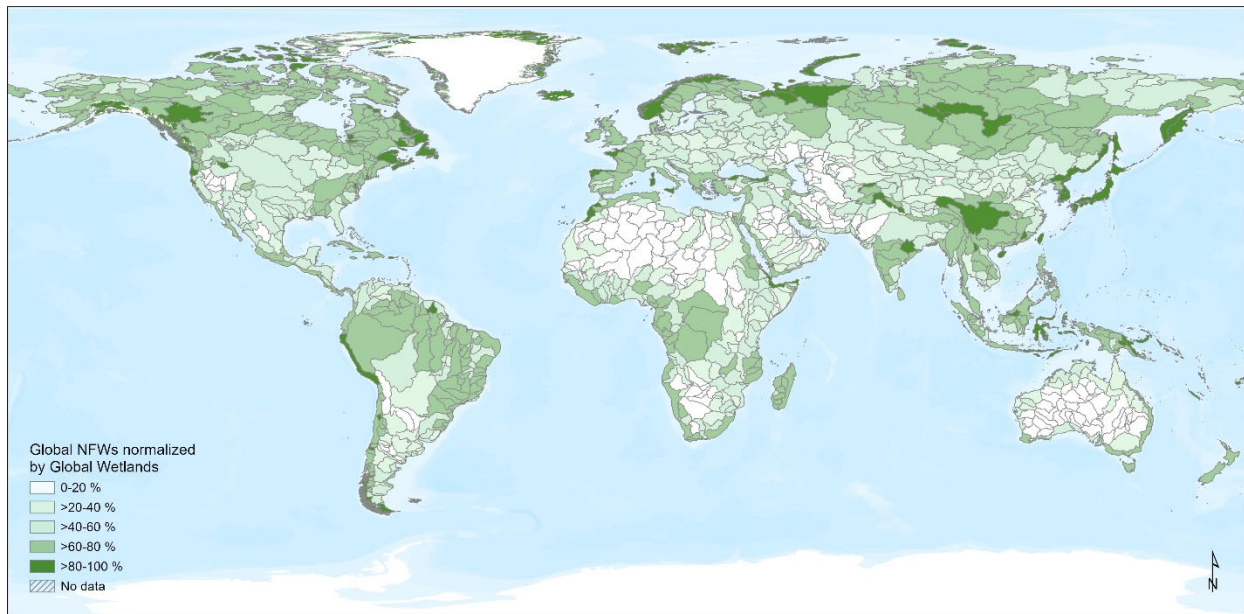
564



565

566 **Figure 6.** Non-floodplain wetlands, Global NFWs, are found worldwide, with a greater abundance in formerly  
567 glaciated landscapes of northern climates (e.g., northern North America and Siberian Russia) as well as within the  
568 Amazon basin (South America). This density map was created using the Focal Statistics tool in ArcGIS Pro 2.9.1.  
569 The basemap layer is the ESRI World Terrain Base (2022).





571

572 **Figure 7.** The proportion of non-floodplain wetlands, Global NFWs, within a given HydroBASINS watershed  
 573 (Lehrner and Grill, 2013), ranging up to 100 %, varied globally. The impacts or effects of non-floodplain wetlands  
 574 on biological, biogeochemical, and hydrological functions will vary based on their relative abundance, location  
 575 within the watershed, and hydrologic characteristics (Lane et al., 2018). The basemap layer is the ESRI World  
 576 Terrain Base (2022).

577

578 floodplain wetlands. Africa (5.4 %) and Greenland (1.0 %, excluding ice sheets) had the least abundance  
 579 of non-floodplain wetlands. A four-direction region-group (contagion) analysis conducted to identify  
 580 adjacent pixels considered as contiguous units or non-floodplain wetland systems identified 32.8 million  
 581 individual non-floodplain wetlands. Non-floodplain wetlands are typically small aquatic systems (see  
 582 Table 7): the median size differed across the HydroBASINS regions from 0.018 km<sup>2</sup> (1.8 ha) to 0.138  
 583 km<sup>2</sup> (13.8 ha) with a global median of 0.039 km<sup>2</sup> (3.87 ha).

584 **Table 7.** Global NFW data further described by HydroBASINS region.

<b>HydroBASINS Region</b>	<b>Global NFW Extent (km<sup>2</sup>)</b>	<b>Count of Global NFWs (#)</b>	<b>Global NFW Percent of Landmass</b>	<b>Global NFW Median Area (km<sup>2</sup>)</b>
<b>Africa</b>	1,611,225	2,698,465	5.4 %	0.138
<b>Arctic (northern Canada &amp; Alaska)</b>	1,371,937	5,956,081	21.7 %	0.018
<b>Asia</b>	2,924,900	4,564,172	14.0 %	0.049
<b>Australasia</b>	850,402	1,448,315	7.6 %	0.054
<b>Europe and Middle East</b>	1,475,355	3,740,961	8.3 %	0.054
<b>Greenland (excl. ice sheet)</b>	21,747	180,726	1.0 %	0.018
<b>North &amp; Central America (excl. Alaska)</b>	2,608,158	5,740,066	16.4 %	0.025
<b>Siberian Russia</b>	2,255,689	4,864,577	17.4 %	0.063
<b>South America</b>	2,891,604	3,572,294	16.2 %	0.096
<b>Total</b>	16,011,018	32,765,657	11.9 %	0.039

585

586 **4 Discussion**

587

588 We report here for the first time the global abundance of non-floodplain wetlands, a functionally  
 589 important and imperiled resource (Creed et al., 2017). Our estimate of 16.0 million km<sup>2</sup> suggests that  
 590 approximately 53 % of the Earth’s wetlands are likely non-floodplain wetland systems. These aquatic  
 591 systems are small, with a range from 0.018-0.138 km<sup>2</sup> (1.8-13.8 ha) across the globe and a global median  
 592 size of 0.039 km<sup>2</sup> (3.87 ha, see Table 7).

593

594 The global abundance of non-floodplain wetlands is a reasonable first approximation of the total non-  
 595 floodplain wetland extent. For instance, non-floodplain wetland estimates in the CONUS were conducted  
 596 by Lane et al. (2022) using high-resolution aerial-sourced spatial data layers developed by the National  
 597 Wetlands Inventory (U.S. Fish and Wildlife Service, various dates). Lane et al. (2022) reported  
 598 approximately 23% of the area of freshwater wetlands to be non-floodplain wetland systems. Yet the  
 599 CONUS has lost nearly half of its wetlands since the European colonization (Dahl, 1990), with smaller  
 600 and shallower non-floodplain wetlands likely being disproportionately lost (Van Meter and Basu, 2015;  
 601 Serran et al., 2017).

602



603 Tootchi et al. (2019) – our base input geospatial data layer – calculated that the global wetland extent  
604 identified from incorporating both regularly flooded wetland systems (surface-water and precipitation-  
605 sourced) and groundwater-driven wetland systems (e.g., Fan et al., 2013; Hu et al., 2017b) resulted in  
606 approximately 27.5 million km<sup>2</sup> of wetlands, a value towards the higher-end of previously published  
607 geospatial wetland datasets (Hu et al., 2017a). In their synthesis, Tootchi et al. (2019) explained their  
608 values as particularly influenced by groundwater-driven wetlands, especially those in the tropics (10° N-  
609 10° S latitudes, Zhu et al., 2022), following recent studies acknowledging the under-estimation of those  
610 wetland systems (e.g. Wania et al., 2013; Gumbrecht et al., 2017).

611  
612 It follows that incorporating additional higher-resolution satellite inundation data (Pekel et al., 2016) as  
613 well as groundwater-driven wetland systems data (e.g., Fan et al., 2013; Tootchi et al., 2019), as  
614 conducted in this study, would similarly maintain the trend towards the higher end in global estimates as  
615 found by Hu et al. (2017a) and Tootchi et al. (2019). This is meted out in the simple contrast between the  
616 proportional abundance of non-floodplain wetland systems identified here against the 30 m NLCD data  
617 product described above (Dewitz, 2019) across the 21 CONUS watersheds in this study. The calculated  
618 median watershed abundance of non-floodplain wetlands in both the Global NFWs (9.4 %) and the  
619 Tootchi et al. (2019) CW-WTD (9.1 %) datasets from our validation watersheds are nearly 5-fold the  
620 abundance of the benchmark data from the NLCD (Table 8). However, this is contrasted with a 7-fold  
621 *under-representation* of non-floodplain wetlands as derived from the satellite based GSW data (Table 8,  
622 Pekel et al., 2016). This suggests that our first approximation of global non-floodplain wetland estimates  
623 may be high, primarily due to the resolution of the input data layers. However, as we discuss below,  
624 additional factors than just resolution are likely at play.

625  
626 It is apparent that the GSW alone is insufficient to map non-floodplain wetlands (this study, Vanderhoof  
627 and Lane, 2019). Though useful as a satellite-based input data layer, the GSW by itself appears  
628 inadequate for identifying non-floodplain wetlands because it relies on surface-water inundation and

629 ignores saturated wetland systems and those driven by groundwater discharge and upwelling (Winter et  
630 al., 1998). Fan et al. (2013) found that groundwater drivers of aquatic system state were important and  
631 underrepresented in global datasets. Relying on surface water inundation captured during satellite  
632 overflights depends not only on an unobstructed view of the waterbody (e.g., not obscured by trees) but  
633 also fortuitous timing regarding inundation status. For example, in an analysis of non-floodplain wetlands  
634 of the CONUS as derived by distance from an aquatic system, Lane and D'Amico (2016) reported that  
635 just over 50 % of the non-floodplain wetlands were classified as seasonally or temporarily flooded –  
636 meaning that cloud-free and unobscured overflights would only potentially identify these systems at  
637

638 **Table 8.** A comparison of the non-floodplain wetland distribution within the 21 HUCs contrasting across NLCD  
639 (the benchmark data layer, Dewitz, 2019), Global NFW (this study), CW-WTD (Tootchi et al., 2019), and GSW  
640 (Pekel et al., 2016). The CW-WTD (at 500 m) and the Global NFW (coupling 500 m, 300 m, and 30 m data),  
641 derived from the CW-WTD, identified 5-fold the abundance of non-floodplain wetlands whereas the GSW under-  
642 estimated non-floodplain wetlands nearly 7-fold.

HUC ID	Percent HUC as			
	NLCD NFW	Global NFW	CW-WTD NFW	GSW NFW
HUC_0101	10.4 %	19.2 %	18.9 %	0.1 %
HUC_0103	8.1 %	14.6 %	14.3 %	0.2 %
HUC_0106	8.2 %	8.0 %	7.5 %	0.3 %
HUC_0203	4.9 %	8.4 %	8.3 %	0.4 %
HUC_0208	4.7 %	12.0 %	11.5 %	4.6 %
HUC_0304	12.2 %	21.7 %	20.8 %	12.2 %
HUC_0313	8.3 %	14.4 %	13.5 %	8.2 %
HUC_0501	1.5 %	9.2 %	8.9 %	0.1 %
HUC_0706	0.7 %	9.7 %	9.5 %	0.3 %
HUC_0804	9.7 %	17.1 %	16.2 %	9.7 %
HUC_1003	0.7 %	2.1 %	1.9 %	0.2 %
HUC_1015	1.8 %	2.0 %	1.3 %	0.1 %
HUC_1016	3.6 %	16.6 %	15.5 %	2.6 %
HUC_1024	0.5 %	5.1 %	4.9 %	0.2 %
HUC_1029	0.9 %	8.4 %	7.7 %	0.4 %
HUC_1304	0.0 %	5.5 %	5.5 %	0.0 %
HUC_1601	0.7 %	1.3 %	1.0 %	0.1 %
HUC_1708	2.0 %	11.7 %	11.6 %	0.4 %
HUC_1711	1.8 %	9.4 %	9.1 %	0.2 %
HUC_1805	2.2 %	9.9 %	9.7 %	0.5 %
HUC_1808	0.3 %	1.7 %	1.6 %	0.1 %
<b>Median</b>	2.0 %	9.4 %	9.1 %	0.3 %

643

644 certain inundated times of the year. Additionally, Lane and D'Amico (2016) identified another 6 % of  
645 CONUS non-floodplain wetlands as saturated (i.e., wetlands with saturated substrates but with surface  
646 water seldom present). These wetlands would not be identified by the GSW (Pekel et al., 2016) resulting  
647 in a further under-representation of the global resource. Similarly, Hamunyela et al. (2022), analyzing  
648 ~150,000 km<sup>2</sup> in southeastern Africa, found that the GSW underestimated surface water extent (i.e.,  
649 omission errors) by nearly 65%. Vanderhoof and Lane (2019) found approximately 42% omission rates  
650 when contrasting the GSW data to surface-water extent in non-floodplain wetlands ranging from 0.2-17.6  
651 ha in area in the Midwestern US. While the GSW is an outstanding dataset that is continuing to be  
652 managed and updated, the GSW and its derived product have limitations in their stand-alone utility in  
653 global non-floodplain wetland analyses.

654  
655 While solely using satellite-based surface-water data products omits groundwater-driven and saturated  
656 wetlands and likely results in non-floodplain wetland underestimations, our Global Wetland data  
657 incorporated the finer-resolution CCI (Herold et al., 2015) and GSW (Pekel et al., 2016) products into the  
658 Tootchi et al. (2019) base map, substantially improving wetland identification (see Table 3). These  
659 improvements, as indicated by performance indices increasing from 10-50 % in the derived Global NFW  
660 data (see Table 4), support the inclusion of these higher-resolution satellite-based data (Herold et al.,  
661 2015; Pekel et al., 2016) with groundwater datasets (Fan et al., 2013), especially when focused on smaller  
662 and non-floodplain wetland systems. Similarly, at a coarser scale of 1 km, there was a difference in Mean  
663 Absolute Error value of 0.09 (see Table 4) between the Global NFWs and the benchmark NLCD. This ~9  
664 % difference between the two datasets at a 1 km resolution (the former originating at 500 m and the latter  
665 at 30 m) further suggest substantive potential utility in these global non-floodplain wetland data for  
666 effective natural resource management and decision-making.

667

668

## 669 5 Implications

670  
671 Non-floodplain wetlands remain vulnerable waters (Creed et al., 2017), despite the fact that the  
672 hydrological, biogeochemical, and biological functions performed by non-floodplain wetlands are  
673 increasingly noted in the literature (e.g., Leibowitz, 2003; Creed et al., 2017; Lane et al., 2018; Lane et  
674 al., 2022), incorporated into eco-hydrological models by the scientific community (e.g., Fossey and  
675 Rousseau, 2016; Golden et al., 2017; Golden et al., 2021; Leibowitz et al., 2023), and considered by  
676 policy makers (e.g., Biggs et al., 2017; Drenkhan et al., 2022). Their global fate has important  
677 implications for watershed-scale resilience to changing climatic conditions (Mckenna et al., 2017; Lane et  
678 al., 2022) affecting the measured benefits humans receive from biogeochemical processing, stormwater  
679 attenuation, and drought mitigation functions provided by non-floodplain wetlands.

680  
681 Global attention to functions of non-floodplain wetlands has increased in the United States (Marton et al.,  
682 2015; Rains et al., 2016; Cohen et al., 2016), Europe (Biggs et al., 2017; Nitzsche et al., 2017; Rodríguez-  
683 Rodríguez et al., 2021), Asia (Kam, 2010; Van Meter et al., 2014), Australia (Adame et al., 2019), Africa  
684 (Merken et al., 2015; Samways et al., 2020), South America (Rodrigues et al., 2012; Cunha et al., 2019)  
685 and elsewhere (see extensive review in Chen et al., 2022). This includes analyses of non-floodplain  
686 wetlands both as individual systems (e.g., assessing the functions of a single wetland or wetland complex;  
687 Badiou et al., 2018) as well as agglomerated, watershed-scale functioning systems (e.g., answering  
688 questions on the functional contributions of all non-floodplain wetlands at larger spatial extents; Golden  
689 et al., 2016; Blanchette et al., 2022). Previous studies found that non-floodplain wetlands are  
690 overwhelmingly important contributors to biogeochemical and hydrological functions affecting  
691 downgradient (i.e., down-stream) water quality and streamflow (e.g., McLaughlin et al., 2014; Marton et  
692 al., 2015; Cohen et al., 2016; Rains et al., 2016; Golden et al., 2019; Cheng et al., 2020). Hence, with the  
693 development of this publicly available dataset, and subsequent improvements by others, it is hoped that

694 these important aquatic systems will be incorporated into resource management and decision-making  
695 across the globe.

696  
697 Recently, Lane et al. (2022) identified global-scale geospatial data of the spatial extent and spatial  
698 configuration of vulnerable waters – non-floodplain wetlands and headwater stream systems (e.g.,  
699 ephemeral, intermittent, and perennial low-order waters [Strahler, 1957]) – as a critical scientific gap.  
700 Discounting their significance in watershed-scale hydrology and nutrient biogeochemistry analyses – as  
701 well as their importance in biological processes (Schofield et al., 2018; Smith et al., 2019; Mushet et al.,  
702 2019) – affects quantification of the myriad ecosystem services they provide (De Groot, 2006; Colvin et  
703 al., 2019). For instance, Golden et al. (2021) provide a tangible example of the functional effects and  
704 influence of non-floodplain wetlands once incorporated into watershed-scale hydrologic models (Fig. 8):  
705 ignoring non-floodplain wetlands in the model resulted in projected critical flood-stage return intervals  
706 (e.g., 50 yr and 100 yr floods) being reached within a given modeled time frame. Conversely,  
707 incorporating non-floodplain wetlands and their storage capacities into a river basin model (e.g., Rajib et  
708 al., 2020) demonstrated that non-floodplain wetlands significantly attenuate storm flows, for when non-  
709 floodplain wetlands are “...integrated into the model, those simulated *flood stages are not reached*”  
710 (Golden et al., 2021, p. 3, emphasis added). The hydrological functions and concomitantly the associated  
711 biogeochemical functions (e.g., Marton et al., 2015) of non-floodplain wetlands demand an effective  
712 accounting of their spatial extent and configuration, as demonstrated in this novel global dataset.

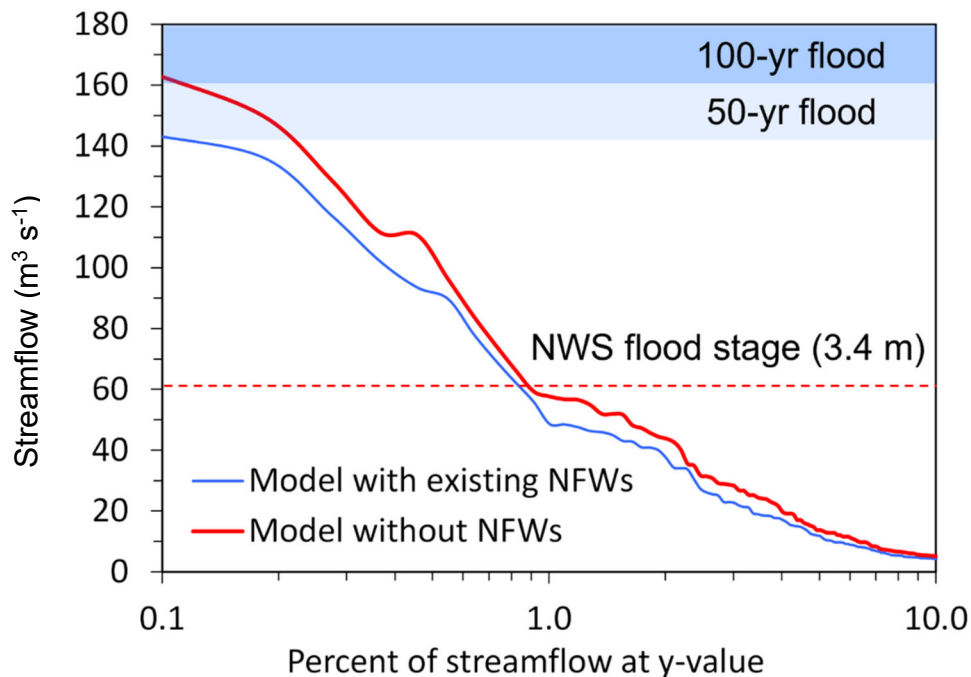
713

## 714 **6 Global Non-Floodplain Wetlands: Continuing advancements and conclusion**

715

716 Noting the challenges in accurately identifying non-floodplain wetlands – including small size, frequent  
717 non-perennial hydrological inundation, soil saturation rather than overlying surface water, and canopy or  
718 cloud cover obstructing satellite or airborne detection – recommendations for advanced analyses of non-  
719 floodplain wetland extent hinge initially on the use of ancillary data sources. For instance, global

720 assessments will be improved through wall-to-wall high resolution digital elevation models that are used  
 721 to identify depressions on the landscape (e.g., Wu et al., 2019b). Though not all landscape depressions are  
 722 non-floodplain wetlands (or wetlands at all), analyses that include depressions may find improved  
 723 performance when used in combination with vegetation-based assessments or spectral analyses  
 724 identifying water (Devries et al., 2017; Evenson et al., 2018b). Similarly, emerging synthetic aperture  
 725 radar-based landscape classifications (e.g., Huang et al., 2018; Martinis et al., 2022; Brown et al., 2022)  
 726 and both airborne and satellite-borne hyperspectral and advanced analyses, including LiDAR, as well as  
 727  
 728



729  
 730 **Figure 8.** Non-floodplain wetlands attenuate storm flows and decrease flooding hazards. In this example from  
 731 Golden et al. (2021, used by permission under Creative Commons Attribution 4.0 license), incorporating the  
 732 floodwater storage and attenuation functions of non-floodplain wetlands (NFWs, here) resulted in substantive  
 733 decreases in flood-stage heights (i.e., modeled stream outcomes incorporating non-floodplain wetlands reached  
 734 neither 50 yr nor 100 yr floods extents). The data from Golden et al. (2021) is of USGS Pipestem Creek gage  
 735 06469400, draining approximately 1,800 km<sup>2</sup>.

736 analytical capabilities (e.g., machine-learning approaches, object-oriented classifications, Berhane et al.,  
737 2018); topographically based models, Xi et al., 2022; see Table B1) hold great promise for improved  
738 resolution and performance in identifying non-floodplain wetlands (Christensen et al., 2022).

739

740 The Global NFW dataset is not perfect, yet it incrementally advances the current understanding of the  
741 potential extent of this important aquatic resource. Limitations of the global dataset (see also Section 4)  
742 include the error-propagation and imperfections of the input data layers, including the relatively coarse  
743 nature of four of the main input data layers (i.e., the 1000 m groundwater data from Fan et al. (2013), 500  
744 m CW-WTD from Tootchi et al. (2019), 500 m GIEMS-D15 from Fluet-Chouinard et al. (2015), and the  
745 300 m CCI from Herold et al. (2015)) relative to the target wetland size as clearly evident in Fig. 4. We  
746 additionally acknowledge that omission and commission errors remain within this global data product.  
747 For instance, our floodplain-masking process may have inadvertently misassigned pixels derived at 500 m  
748 into either non-floodplain or floodplain groups. Though data were not lost when we resampled  
749 downwards to 30 m from 500 m, the topological relationships were not necessarily maintained, adding  
750 error to the determination of floodplain or non-floodplain pixel status (especially as it relates to those  
751 pixels proximate to floodplains). Though imperfect, we suggest Global NFW data should be cautiously  
752 incorporated into hydrological, biogeochemical, and biological models to account for the important  
753 functions non-floodplain wetlands perform.

754

755 Similarly, though this Global NFW is a static data layer, land use, development, and climate changes  
756 continue to affect the prevalence of wetlands worldwide. Fluet-Chouinard et al. (2023) recently noted a  
757 global wetland loss of 21% since 1700, with rapid increases from 1950s onwards. Returning to the  
758 identification of wetlands and their spatial location vis-à-vis floodplains, using the preponderance of  
759 higher-resolution (i.e., < 30 m) and high-return interval sensors will improve both the spatial and  
760 temporal accuracy of these data, decreasing commission and omission errors (e.g., Table 8) while

761 increasing the accurate identification of smaller aquatic features that occasional cease to hold standing  
762 water.

763  
764 The keys to quantifying the functional contributions, ecosystem services, and watershed-scale resilience  
765 conferred by non-floodplain wetlands through hydrological, biogeochemical, and biological processes are  
766 found through, as a first principle, identifying the spatial extent and configuration of this disappearing and  
767 imperiled aquatic system (Creed et al., 2017; Lane et al., 2022). This novel geospatial dataset, freely  
768 available ([https://gaftp.epa.gov/EPADDataCommons/ORD/Global\\_NonFloodplain\\_Wetlands/](https://gaftp.epa.gov/EPADDataCommons/ORD/Global_NonFloodplain_Wetlands/), Lane et al.,  
769 2023), provides for sustainable management of an important aquatic resource and advances the global  
770 assessment of non-floodplain wetland functions by facilitating non-floodplain wetland inclusion in both  
771 existing models and those under development (Golden et al., 2021).

772

## 773 **7 Data availability**

774

775 The data are available on the United State Environmental Protection Agency’s Environmental Dataset  
776 Gateway (DOI: <https://doi.org/10.23719/1528331>, Lane et al., 2023) or  
777 [https://gaftp.epa.gov/EPADDataCommons/ORD/Global\\_NonFloodplain\\_Wetlands/](https://gaftp.epa.gov/EPADDataCommons/ORD/Global_NonFloodplain_Wetlands/), (last accessed  
778 12/06/2022). Here, we provide global gridded floodplain (90 m, GFPLain90, ~/Global\_Floodplains),  
779 global gridded wetlands (30 m, Global Wetlands, ~/Global\_Wetlands), and global gridded non-floodplain  
780 wetlands (30 m, Global NFWs, ~/Global\_NFWs) for each of the 3142 HydroBASINS, organized by  
781 HydroBASINS region (see, e.g., Table 7).

782

783 **Author contributions.** CL, JC, HG, and ED conceptualized the study, developed the formal analysis, and  
784 conducted and/or assisted the data validation. CL wrote and edited the manuscript, while JC and HG  
785 reviewed and edited the manuscript. ED also developed the methodology, curated the data, conducted the  
786 formal spatial analysis, validated the data, visualized the data, and reviewed and edited the manuscript.



787 QW and AR assisted in methodology development, validated the study outputs, conducted formal  
788 analyses, and reviewed and edited the manuscript.

789  
790 **Competing interests.** The corresponding authors have declared that none of the authors have any  
791 competing interests.

792  
793 **Disclaimer.** Publisher’s note: Copernicus Publications remains neutral with regard to jurisdictional  
794 claims in published maps and institutional affiliations.

795  
796 **Acknowledgements.** We greatly appreciate the scientific contributions and stimulative discussions in the  
797 papers led by Ardalan Tootchi, Sean Woznicki, Fernando Nardi, Oliver Wing, Paul Bates, and their co-  
798 authors that inspired us to complete these analyses. Jeremy Baynes and John Johnston conducted critical  
799 reviews to improve this manuscript, and their efforts are acknowledged. This paper has been reviewed in  
800 accordance with the US Environmental Protection Agency’s peer and administrative review policies and  
801 approved for publication. Mention of trade names or commercial products does not constitute  
802 endorsement or recommendation for use. Statements in this publication reflect the authors’ professional  
803 views and opinions and should not be construed to represent any determination or policy of the US  
804 Environmental Protection Agency.

805  
806 **Review statement.** This paper was edited by Yuanzhi Yao and reviewed by Youjiang Shen and Michele  
807 Ronco.

808  
809 **Appendix A: Abbreviations**

810	AEB	Aggregate error bias
811	CaMa-Flood	Catchment-based Macro-scale Floodplain
812	CCI	Climate change initiative

813	CIMA-UNEP	CIMA Research Foundation - United Nations Environmental Programme
814	CONUS	Conterminous United States
815	CSI	Critical Success Index
816	CW-WTD	Composite wetland-water table depth
817	DEM	Digital elevation model
818	EB	Error Bias
819	ECMWF	European Centre for Medium-Range Weather Forecasts
820	EPA	Environmental Protection Agency
821	ESA	European Space Agency
822	FA	False Alarm
823	FEMA	Federal Emergency Management Agency
824	GDW	Groundwater-driven wetlands
825	GFPlain	Global Floodplain
826	GIEMS-D15	Global Inundation Extent from Multi-Satellites Downscaled - 15 arcseconds
827	GIS	Geographic information systems
828	GLOFRIS	Global Flood Risk with Image Scenarios
829	GLWD	Global Lakes and Wetlands Database
830	GNFW	Global Non-floodplain wetlands
831	GSW	Global surface water
832	GW	Global wetlands
833	H	Hit Rate
834	HUC	Hydrologic unit code
835	IPCC	Intergovernmental Panel on Climate Change
836	JRC	Joint Research Center
837	LIDAR	Light detection and ranging
838	MAE	Mean absolute error

839	MERIT	Multi-Error Removed Improved Terrain
840	ML	Machine learning
841	NFW	Non-floodplain wetland
842	NLCD	National Land Cover Database
843	NWS	National Weather Service
844	P	Precision
845	RFW	Regularly flooded wetland
846	SAR	Synthetic aperture radar
847	USA	United States of America
848	USGS	United States Geological Survey
849	UTM	Universal Transverse Mercator
850	WTD	Water table depth
851		

852 **Appendix B: Supplemental Tables and Figures**

853 **Table B1.** Emerging global land cover datasets related to surface water and wetlands.

<b>Data Set</b>	<b>Resolution</b>	<b>Years of Data</b>	<b>Wetland Classes</b>	<b>Image Sources</b>	<b>Reference and website</b>
ESA WorldCover	10 m	2020-2021	Permanent water bodies; herbaceous wetland; mangroves	Sentinel-1 & Sentinel-2	Zanaga et al. (2021); <a href="https://esa-worldcover.org">https://esa-worldcover.org</a>
Esri Global Land Cover	10 m	2017-2022	Water; flooded vegetation	Sentinel-2	Karra et al. (2021); <a href="https://livingatlas.arcgis.com/landcover">https://livingatlas.arcgis.com/landcover</a>
Dynamic World	10 m	2015-2023	Water; flooded vegetation	Sentinel-2	Brown et al. (2022); <a href="https://dynamicworld.app/">https://dynamicworld.app/</a>

854

855

856 **Table B2.** Descriptive characteristics of the 21 verification basins located throughout the CONUS (see Fig. 2).  
857 Majority Köppen-Geiger classification follows Beck et al. (2018). Climatological data were acquired from the  
858 PRISM Climate Group (Parameter-elevation Regressions on Independent Slopes Model, prism.oregonstate.edu/,  
859 accessed 09/26/2022) using the 30-year annual normals for each watershed. Land use data and descriptions are from  
860 the 2019 NLCD (www.mrlc.gov/data, accessed 09/26/2022) and represent the land use class with the greatest areal  
861 abundance. Average elevation was derived from the USGS National Elevation Dataset (https://www.usgs.gov/3d-  
862 elevation-program, accessed 01/13/2022). Global Wetland Count are the counts of wetlands from the derived Global  
863 Wetland database within each watershed after region-grouping the data using a four-direction contagion criterion  
864 (i.e., pixels immediately adjacent in any of the four cardinal directions are considered part of a unique, multi-pixel  
865 wetland, ArcGIS Pro v.2.9.1, Redlands, California).

Hydrologic Unit Code	Area	Köppen-	Mean Annual	Mean Annual
ID	(km <sup>2</sup> )	Geiger	Temp (°C)	Rainfall (m)
HUC_0101	18,906	Dfb	4.0	1.1
HUC_0103	15,287	Dfb	5.4	1.2
HUC_0106	10,800	Dfb	7.5	1.3
HUC_0203	12,490	Dfa	11.6	1.2
HUC_0208	47,449	Cfa	13.7	1.2
HUC_0304	47,899	Cfa	16.4	1.3
HUC_0313	52,169	Cfa	18.1	1.4
HUC_0501	30,371	Dfb	8.6	1.2
HUC_0706	22,257	Dfa	8.1	1.0
HUC_0804	53,108	Cfa	17.5	1.4
HUC_1003	51,431	BSk	5.6	0.4
HUC_1015	37,098	Dfa	8.7	0.5
HUC_1016	54,743	Dfa	6.4	0.6
HUC_1024	35,237	Dfa	10.8	0.9
HUC_1029	48,204	Dfa	13.2	1.1
HUC_1304	48,126	BSh	18.6	0.4
HUC_1601	19,463	BSk	5.7	0.5
HUC_1708	16,101	Csb	9.0	2.1
HUC_1711	35,651	Csb	8.2	2.0
HUC_1805	11,341	Csb	14.9	0.7
HUC_1808	11,789	BSk	8.4	0.4

866 † Köppen-Geiger Class Descriptions (Beck et al. 2018): BSh (arid, steppe, hot), BSk (arid, steppe, cold), Cfa  
867 (temperate, no dry season, hot summer), Csb, (temperature, dry season, warm summer), Dfa (cold, no dry season,  
868 hot summer), Dfb (cold, no dry season, warm summer)

869

870 **Table B2.** (Continued)

<b>Hydrologic Unit</b>	<b>Majority Land</b>	<b>Majority Land</b>	<b>Global Wetland</b>	<b>Average</b>
<b>Code</b>	<b>Use Coverage</b>	<b>Coverage Description</b>	<b>Count</b>	<b>Elevation</b>
<b>HUC_0101</b>	43	Mixed Forest	2,141	296
<b>HUC_0103</b>	43	Mixed Forest	2,202	300
<b>HUC_0106</b>	43	Mixed Forest	2,799	169
<b>HUC_0203</b>	41	Deciduous Forest	2,438	82
<b>HUC_0208</b>	41	Deciduous Forest	13,934	187
<b>HUC_0304</b>	90	Woody Wetlands	14,643	127
<b>HUC_0313</b>	42	Evergreen Forest	27,056	147
<b>HUC_0501</b>	41	Deciduous Forest	6,310	484
<b>HUC_0706</b>	82	Cultivated Crops	3,100	300
<b>HUC_0804</b>	42	Evergreen Forest	12,242	85
<b>HUC_1003</b>	71	Herbaceous	11,852	1349
<b>HUC_1015</b>	71	Herbaceous	8,628	961
<b>HUC_1016</b>	82	Cultivated Crops	61,482	464
<b>HUC_1024</b>	82	Cultivated Crops	11,995	341
<b>HUC_1029</b>	81	Hay/Pasture	23,935	297
<b>HUC_1304</b>	52	Shrub/Scrub	1,733	995
<b>HUC_1601</b>	52	Shrub/Scrub	2,642	1981
<b>HUC_1708</b>	42	Evergreen Forest	1,986	552
<b>HUC_1711</b>	42	Evergreen Forest	6,562	621
<b>HUC_1805</b>	52	Shrub/Scrub	1,208	222
<b>HUC_1808</b>	52	Shrub/Scrub	1,089	1625

871

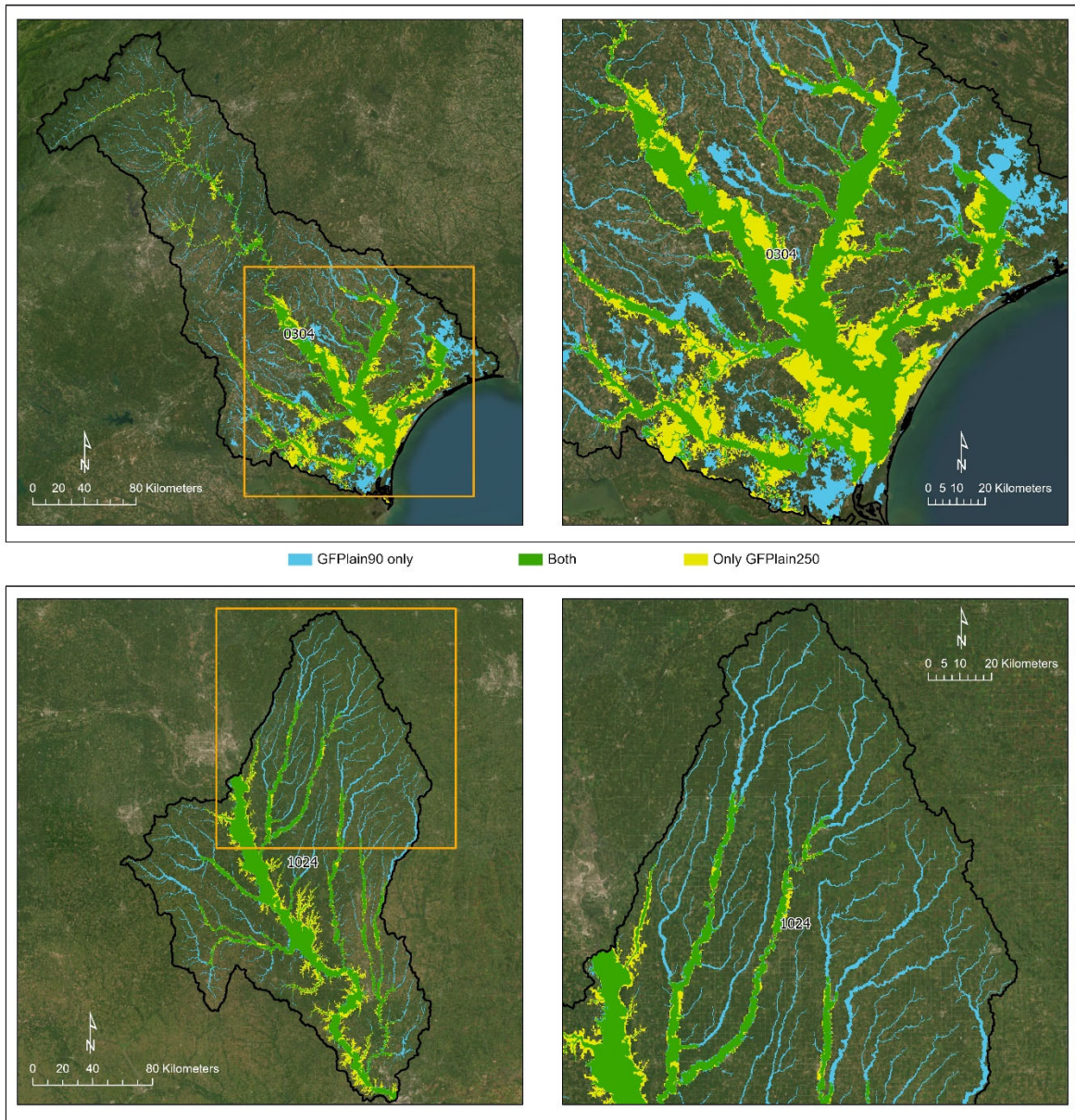
872

873 **Table B3.** Floodplain performance assessment of the GFPlain90-derived floodplain and the benchmark floodplain  
874 from Woznicki et al. (2019). The first six equations directly assess the spatial concordance and overlap between the  
875 two datasets, whereas Mean Absolute Error (Eq. 7) and Aggregate Error Bias (Eq. 8) are coarser fractional analyses  
876 (i.e., the fraction of a 1 km<sup>2</sup> cell predicted correctly) as measured along the riverine network.

Hydrologic Unit Code (HUC) ID	Hit Rate	Precision	False Alarm	CSI	F1	Error Bias	Mean Absolute Error	Aggregate Error Bias
	(Eq. 1)	(Eq. 2)	(Eq. 3)	(Eq. 4)	(Eq. 5)	(Eq. 6)	(Eq. 7)	(Eq. 8)
HUC_0101	0.76	0.84	0.16	0.66	0.80	0.62	0.06	-0.01
HUC_0103	0.92	0.77	0.23	0.72	0.84	3.25	0.05	0.03
HUC_0106	0.78	0.74	0.26	0.62	0.76	1.24	0.10	-0.03
HUC_0203	0.47	0.58	0.42	0.35	0.52	0.66	0.25	-0.18
HUC_0208	0.64	0.73	0.27	0.52	0.68	0.67	0.13	-0.08
HUC_0304	0.63	0.81	0.19	0.55	0.71	0.41	0.06	0.00
HUC_0313	0.62	0.72	0.28	0.50	0.67	0.62	0.09	-0.01
HUC_0501	0.77	0.85	0.15	0.68	0.81	0.59	0.04	-0.02
HUC_0706	0.86	0.79	0.21	0.69	0.82	1.62	0.04	0.02
HUC_0804	0.75	0.83	0.17	0.65	0.79	0.64	0.08	-0.02
HUC_1003	0.85	0.42	0.58	0.39	0.56	7.70	0.11	0.09
HUC_1015	0.81	0.74	0.26	0.63	0.78	1.54	0.06	0.02
HUC_1016	0.89	0.36	0.64	0.35	0.52	14.79	0.18	0.17
HUC_1024	0.90	0.88	0.12	0.80	0.89	1.19	0.03	0.00
HUC_1029	0.84	0.87	0.13	0.75	0.85	0.82	0.04	-0.01
HUC_1304	0.66	0.74	0.26	0.53	0.70	0.67	0.07	-0.01
HUC_1601	0.92	0.55	0.45	0.52	0.69	9.47	0.10	0.08
HUC_1708	0.60	0.71	0.29	0.48	0.65	0.60	0.08	-0.03
HUC_1711	0.70	0.50	0.50	0.41	0.58	2.25	0.10	-0.02
HUC_1805	0.59	0.59	0.41	0.41	0.59	1.00	0.14	-0.05
HUC_1808	0.98	0.44	0.56	0.44	0.61	82.97	0.24	0.23
<b>Median</b>	0.77	0.74	0.26	0.53	0.70	1.00	0.08	-0.01
<b>Mean</b>	0.76	0.69	0.31	0.56	0.71	6.35	0.10	0.01

877

878



879

880 **Figure B1.** Comparison of floodplain extents derived from GFPlain90 (this study) and GFPlain250 (Nardi et al.,  
 881 2019). The right-hand panels are the inset area outlined in the orange box on the left panels; the top panels represent  
 882 an eastern coastal watershed (HUC\_0304) whereas the bottom panels are from a midwestern US watershed  
 883 (HUC\_1024). The full extent of the riverine network is evident in the GFPlain90 dataset, which was derived from 90  
 884 m resolution DEMs in contrast to the 250 m pixel size of the GFPlain250. Satellite imagery sourced from ESRI  
 885 (2022).



886 **References**

887

888 Adame, M. F., Arthington, A. H., Waltham, N., Hasan, S., Selles, A., and Ronan, M.: Managing threats  
889 and restoring wetlands within catchments of the Great Barrier Reef, Australia, *Aquatic Conservation:  
890 Marine and Freshwater Ecosystems*, 29, 829-839, <https://doi.org/10.1002/aqc.3096>, 2019.

891 Alfieri, L., Salamon, P., Bianchi, A., Neal, J., Bates, P., and Feyen, L.: Advances in pan-European flood  
892 hazard mapping, *Hydrological Processes*, 28, 4067-4077, 10.1002/hyp.9947, 2014.

893 Ameli, A. A. and Creed, I. F.: Does Wetland Location Matter When Managing Wetlands for Watershed-  
894 Scale Flood and Drought Resilience?, *JAWRA Journal of the American Water Resources Association*,  
895 55, 529-542, 10.1111/1752-1688.12737, 2019.

896 Aronica, G., Bates, P. D., and Horritt, M. S.: Assessing the uncertainty in distributed model predictions  
897 using observed binary pattern information within GLUE, *Hydrological Processes*, 16, 2001-2016,  
898 <https://doi.org/10.1002/hyp.398>, 2002.

899 Assessment, M. E.: *Ecosystems and Human Well-Being: Wetlands and Water Synthesis*, World  
900 Resources Institute, Washington, D.C., 2005.

901 Badiou, P., Page, B., and Akinremi, W.: Phosphorus Retention in Intact and Drained Prairie Wetland  
902 Basins: Implications for Nutrient Export, *Journal of Environmental Quality*, 47, 902-913,  
903 <https://doi.org/10.2134/jeq2017.08.0336>, 2018.

904 Bam, E. K. P., Ireson, A. M., van der Kamp, G., and Hendry, J. M.: Ephemeral Ponds: Are They the  
905 Dominant Source of Depression-Focused Groundwater Recharge?, *Water Resources Research*, 56,  
906 e2019WR026640, <https://doi.org/10.1029/2019WR026640>, 2020.

907 Bates, P. D. and De Roo, A. P. J.: A simple raster-based model for flood inundation simulation, *Journal of*  
908 *Hydrology*, 236, 54-77, [http://dx.doi.org/10.1016/S0022-1694\(00\)00278-X](http://dx.doi.org/10.1016/S0022-1694(00)00278-X), 2000.

909 Beck, H. E., Zimmermann, N. E., McVicar, T. R., Vergopolan, N., Berg, A., and Wood, E. F.: Present  
910 and future Köppen-Geiger climate classification maps at 1-km resolution, *Scientific Data*, 5, 180214,  
911 10.1038/sdata.2018.214, 2018.

912 Berhane, T., Lane, C., Wu, Q., Autrey, B., Anenkhonov, O., Chepinoga, V., and Liu, H.: Decision-Tree,  
913 Rule-Based, and Random Forest Classification of High-Resolution Multispectral Imagery for Wetland  
914 Mapping and Inventory, *Remote Sensing*, 10, 580, 2018.

915 Biggs, J., von Fumetti, S., and Kelly-Quinn, M.: The importance of small waterbodies for biodiversity  
916 and ecosystem services: implications for policy makers, *Hydrobiologia*, 793, 3-39, 10.1007/s10750-  
917 016-3007-0, 2017.

918 Blanchette, M., Rousseau, A. N., Savary, S., and Foulon, É.: Are spatial distribution and aggregation of  
919 wetlands reliable indicators of stream flow mitigation?, *Journal of Hydrology*, 608, 127646,  
920 <https://doi.org/10.1016/j.jhydrol.2022.127646>, 2022.

921 Brown, C. F., Brumby, S. P., Guzder-Williams, B., Birch, T., Hyde, S. B., Mazzariello, J., Czerwinski,  
922 W., Pasquarella, V. J., Haertel, R., Ilyushchenko, S., Schwehr, K., Weisse, M., Stolle, F., Hanson, C.,  
923 Guinan, O., Moore, R., and Tait, A. M.: Dynamic World, Near real-time global 10 m land use land  
924 cover mapping, *Scientific Data*, 9, 251, 10.1038/s41597-022-01307-4, 2022.

925 Buttle, J. M.: Mediating stream baseflow response to climate change: The role of basin storage,  
926 *Hydrological Processes*, 32, 363-378, 10.1002/hyp.11418, 2018.

927 Chen, J., Chen, J., Liao, A., Cao, X., Chen, L., Chen, X., He, C., Han, G., Peng, S., Lu, M., Zhang, W.,  
928 Tong, X., and Mills, J.: Global land cover mapping at 30m resolution: A POK-based operational  
929 approach, *ISPRS Journal of Photogrammetry and Remote Sensing*, 103, 7-27,  
930 <https://doi.org/10.1016/j.isprsjprs.2014.09.002>, 2015.

931 Chen, W., Thorslund, J., Nover, D. M., Rains, M. C., Li, X., Xu, B., He, B., Su, H., Yen, H., Liu, L.,  
932 Yuan, H., Jarsjö, J., and Viers, J. H.: A typological framework of non-floodplain wetlands for global  
933 collaborative research and sustainable use, *Environmental Research Letters*, 17, 113002, 10.1088/1748-  
934 9326/ac9850, 2022.

935 Cheng, F. Y. and Basu, N. B.: Biogeochemical hotspots: Role of small water bodies in landscape nutrient  
936 processing, *Water Resources Research*, 53, 5038-5056, 10.1002/2016WR020102, 2017.

937 Cheng, F. Y., Van Meter, K. J., Byrnes, D. K., and Basu, N. B.: Maximizing US nitrate removal through  
938 wetland protection and restoration, *Nature*, 588, 625-630, 10.1038/s41586-020-03042-5, 2020.

939 Christensen, J. R., Golden, H. E., Alexander, L. C., Pickard, B. R., Fritz, K. M., Lane, C. R., Weber, M.  
940 H., Kwok, R. M., and Keefer, M. N.: Headwater streams and inland wetlands: Status and advancements  
941 of geospatial datasets and maps across the United States, *Earth-Science Reviews*, 104230,  
942 <https://doi.org/10.1016/j.earscirev.2022.104230>, 2022.

943 Cohen, M. J., Creed, I. F., Alexander, L., Basu, N. B., Calhoun, A. J. K., Craft, C., D'Amico, E.,  
944 DeKeyser, E., Fowler, L., Golden, H. E., Jawitz, J. W., Kalla, P., Kirkman, L. K., Lane, C. R., Lang,  
945 M., Leibowitz, S. G., Lewis, D. B., Marton, J., McLaughlin, D. L., Mushet, D. M., Raanan-Kiperwas,  
946 H., Rains, M. C., Smith, L., and Walls, S. C.: Do geographically isolated wetlands influence landscape  
947 functions?, *Proceedings of the National Academy of Sciences*, 113, 1978-1986,  
948 10.1073/pnas.1512650113, 2016.

949 Colvin, S. A. R., Sullivan, S. M. P., Shirey, P. D., Colvin, R. W., Winemiller, K. O., Hughes, R. M.,  
950 Fausch, K. D., Infante, D. M., Olden, J. D., Bestgen, K. R., Danchy, R. J., and Eby, L.: Headwater  
951 Streams and Wetlands are Critical for Sustaining Fish, Fisheries, and Ecosystem Services, *Fisheries*, 44,  
952 73-91, 2019.

953 Cowardin, L. M., Carter, V., Golet, F. C., and LaRoe, E. T.: Classification of Wetlands and Deepwater  
954 habitats of The United States, Fish and Wildlife Service, Washington DCFWS/OBS-79/31, 1979.

955 Creed, I. F., Lane, C. R., Serran, J. N., Alexander, L. C., Basu, N. B., Calhoun, A. J. K., Christensen, J.  
956 R., Cohen, M. J., Craft, C., D'Amico, E., DeKeyser, E., Fowler, L., Golden, H. E., Jawitz, J. W., Kalla,  
957 P., Kirkman, L. K., Lang, M., Leibowitz, S. G., Lewis, D. B., Marton, J., McLaughlin, D. L., Raanan-  
958 Kiperwas, H., Rains, M. C., Rains, K. C., and Smith, L.: Enhancing protection for vulnerable waters,  
959 *Nature Geoscience*, 10, 809-815, 10.1038/ngeo3041, 2017.

960 Cunha, D. G. F., Magri, R. A. F., Tromboni, F., Ranieri, V. E. L., Fendrich, A. N., Campanhão, L. M. B.,  
961 Riveros, E. V., and Velázquez, J. A.: Landscape patterns influence nutrient concentrations in aquatic

962 systems: citizen science data from Brazil and Mexico, *Freshwater Science*, 38, 365-378,  
963 10.1086/703396, 2019.

964 Dahl, T. E.: *Wetlands - Losses in the United States, 1780's to 1980's*, U.S. Department of Interior, Fish  
965 and Wildlife Service Washington DC, 1990.

966 Davidson, N. C.: How much wetland has the world lost? Long-term and recent trends in global wetland  
967 area, *Marine and Freshwater Research*, 65, 934-941, <http://dx.doi.org/10.1071/MF14173>, 2014.

968 Davidson, N. C., E. Fluet-Chouinard and C. M. Finlayson. 2018. Global extent and distribution of  
969 wetlands: trends and issues. *Marine and Freshwater Research* 69, 4, 620-627, 2018.

970 De Groot, R., M. Stuij, M. Finlayson, and N. Davidson: *Valuing Wetlands: Guidance for Valuing the*  
971 *Benefits Derived from Wetland Ecosystem Services*, Ramsar Convention Secretariat, Gland,  
972 Switzerland and Secretariat of the Convention on Biological Diversity, Montreal, Canada, Gland,  
973 Switzerland Ramsar Technical Report No. 3/CBD Technical Series No. 27, 2006.

974 DeVries, B., Huang, C., Lang, M., Jones, J., Huang, W., Creed, I., and Carroll, M.: Automated  
975 Quantification of Surface Water Inundation in Wetlands Using Optical Satellite Imagery, *Remote*  
976 *Sensing*, 9, 807, 2017.

977 Dewitz, J.: National Land Cover Database (NLCD) 2016 Products: U.S. Geological Survey data release  
978 [dataset], <https://doi.org/10.5066/P96HHBIE>, 2019.

979 Drenkhan, F., Buytaert, W., Mackay, J. D., Barrand, N. E., Hannah, D. M., and Huggel, C.: Looking  
980 beyond glaciers to understand mountain water security, *Nature Sustainability*, 10.1038/s41893-022-  
981 00996-4, 2022.

982 ESA Worldwide Land Cover Mapping: <https://esa-worldcover.org/en>, last access: 22 December 2022.  
983 ESA Land Cover CCI, Product User Guide Version 2.0:  
984 [https://maps.elie.ucl.ac.be/CCI/viewer/download/ESACCI-LC-Ph2-PUGv2\\_2.0.pdf](https://maps.elie.ucl.ac.be/CCI/viewer/download/ESACCI-LC-Ph2-PUGv2_2.0.pdf), last access: May  
985 2022.

986 ESRI World Terrain Base  
987 <https://www.arcgis.com/home/item.html?id=be2e229ffc864c868a78f5ca68ca5b8e>, last accessed 22  
988 December 2022.

989 Evenson, G. R., Golden, H. E., Lane, C. R., McLaughlin, D. L., and D'Amico, E.: Depressional Wetlands  
990 Affect Watershed Hydrological, Biogeochemical, and Ecological Functions, *Ecological Applications*,  
991 28, 953-966, 10.1002/eap.1701, 2018a.

992 Evenson, G. R., Jones, C. N., McLaughlin, D. L., Golden, H. E., Lane, C. R., DeVries, B., Alexander, L.  
993 C., Lang, M. W., McCarty, G. W., and Sharifi, A.: A watershed-scale model for depressional wetland-  
994 rich landscapes, *Journal of Hydrology X*, 1, 100002, <https://doi.org/10.1016/j.hydroa.2018.10.002>,  
995 2018b.

996 Evenson, G. R., Golden, H. E., Christensen, J. R., Lane, C. R., Rajib, A., D'Amico, E., Mahoney, D. T.,  
997 White, E., and Wu, Q.: Wetland restoration yields dynamic nitrate responses across the Upper  
998 Mississippi river basin, *Environmental Research Communications*, 3, 095002, 10.1088/2515-  
999 7620/ac2125, 2021.

1000 Fan, Y., Li, H., and Miguez-Macho, G.: Global Patterns of Groundwater Table Depth, *Science*, 339, 940-  
1001 943, doi:10.1126/science.1229881, 2013.

1002 Fewtrell, T. J., Bates, P. D., Horritt, M., and Hunter, N. M.: Evaluating the effect of scale in flood  
1003 inundation modelling in urban environments, *Hydrological Processes*, 22, 5107-5118,  
1004 <https://doi.org/10.1002/hyp.7148>, 2008.

1005 Fluet-Chouinard, E., Lehner, B., Rebelo, L.-M., Papa, F., and Hamilton, S. K.: Development of a global  
1006 inundation map at high spatial resolution from topographic downscaling of coarse-scale remote sensing  
1007 data, *Remote Sensing of Environment*, 158, 348-361, <https://doi.org/10.1016/j.rse.2014.10.015>, 2015.

1008 Fluet-Chouinard, E., B. D. Stocker, Z. Zhang, A. Malhotra, J. R. Melton, B. Poulter, J. O. Kaplan, K. K.  
1009 Goldewijk, S. Siebert, T. Minayeva, G. Hugelius, H. Joosten, A. Barthelmes, C. Prigent, F. Aires, A. M.  
1010 Hoyt, N. Davidson, C. M. Finlayson, B. Lehner, R. B. Jackson and P. B. McIntyre. Extensive global  
1011 wetland loss over the past three centuries, *Nature*, 614, 7947, 281-286, 2023.

1012 Fossey, M. and Rousseau, A. N.: Can isolated and riparian wetlands mitigate the impact of climate  
1013 change on watershed hydrology? A case study approach, *Journal of Environmental Management*,  
1014 184(2):327-339, <http://dx.doi.org/10.1016/j.jenvman.2016.09.043>, 2016.

1015 Golden, H. E., Lane, C. R., Rajib, A., and Wu, Q.: Improving global flood and drought predictions:  
1016 integrating non-floodplain wetlands into watershed hydrologic models, *Environmental Research*  
1017 *Letters*, 16, 091002, 10.1088/1748-9326/ac1fbc, 2021.

1018 Golden, H. E., Rajib, A., Lane, C. R., Christensen, J. R., Wu, Q., and Mengistu, S.: Non-floodplain  
1019 Wetlands Affect Watershed Nutrient Dynamics: A Critical Review, *Environmental Science &*  
1020 *Technology*, 53, 7203-7214, 10.1021/acs.est.8b07270, 2019.

1021 Golden, H. E., Sander, H. A., Lane, C. R., Zhao, C., Price, K., D'Amico, E., and Christensen, J. R.:  
1022 Relative effects of geographically isolated wetlands on streamflow: a watershed-scale analysis,  
1023 *Ecohydrology*, 9, 21-38, 10.1002/eco.1608, 2016.

1024 Golden, H. E., Creed, I. F., Ali, G., Basu, N. B., Neff, B. P., Rains, M. C., McLaughlin, D. L., Alexander,  
1025 L. C., Ameli, A. A., Christensen, J. R., Evenson, G. R., Jones, C. N., Lane, C. R., and Lang, M.:  
1026 Integrating geographically isolated wetlands into land management decisions, *Frontiers in Ecology and*  
1027 *the Environment*, 15, 319-327, 10.1002/fee.1504, 2017.

1028 Gumbricht, T., Roman-Cuesta, R. M., Verchot, L., Herold, M., Wittmann, F., Householder, E., Herold,  
1029 N., and Murdiyarso, D.: An expert system model for mapping tropical wetlands and peatlands reveals  
1030 South America as the largest contributor, *Global Change Biology*, 23, 3581-3599,  
1031 <https://doi.org/10.1111/gcb.13689>, 2017.

1032 Hamunyela, E., Hipondoka, M., Persendt, F., Sevelia Nghiyalwa, H., Thomas, C., and Matengu, K.:  
1033 Spatio-temporal characterization of surface water dynamics with Landsat in endorheic Cuvelai-Etoshia  
1034 Basin (1990–2021), *ISPRS Journal of Photogrammetry and Remote Sensing*, 191, 68-84,  
1035 <https://doi.org/10.1016/j.isprsjprs.2022.07.007>, 2022.

1036 Hoch, J. M. and M. A. Trigg. Advancing global flood hazard simulations by improving comparability,  
1037 benchmarking, and integration of global flood models. *Environmental Research Letters*, 14, 3, 034001,  
1038 2019.

1039 Homer, C., Dewitz, J., Jin, S., Xian, G., Costello, C., Danielson, P., Gass, L., Funk, M., Wickham, J.,  
1040 Stehman, S., Auch, R., and Riitters, K.: Conterminous United States land cover change patterns 2001–  
1041 2016 from the 2016 National Land Cover Database, *ISPRS Journal of Photogrammetry and Remote*  
1042 *Sensing*, 162, 184-199, <https://doi.org/10.1016/j.isprsjprs.2020.02.019>, 2020.

1043 Horritt, M. S. and Bates, P. D.: Evaluation of 1D and 2D numerical models for predicting river flood  
1044 inundation, *Journal of Hydrology*, 268, 87-99, [http://dx.doi.org/10.1016/S0022-1694\(02\)00121-X](http://dx.doi.org/10.1016/S0022-1694(02)00121-X),  
1045 2002.

1046 Hu, S., Niu, Z., and Chen, Y.: Global Wetland Datasets: a Review, *Wetlands*, 37, 807-817,  
1047 [10.1007/s13157-017-0927-z](https://doi.org/10.1007/s13157-017-0927-z), 2017a.

1048 Hu, S., Niu, Z., Chen, Y., Li, L., and Zhang, H.: Global wetlands: Potential distribution, wetland loss, and  
1049 status, *Science of The Total Environment*, 586, 319-327,  
1050 <http://dx.doi.org/10.1016/j.scitotenv.2017.02.001>, 2017b.

1051 Huang, W., DeVries, B., Huang, C., Lang, M., Jones, J., Creed, I., and Carroll, M.: Automated Extraction  
1052 of Surface Water Extent from Sentinel-1 Data, *Remote Sensing*, 10, 797, 2018.

1053 IPCC: Intergovernmental Panel on Climate Change 2014: Impacts, adaptation, and vulnerability,  
1054 Cambridge University Press, Cambridge, U.K.2014.

1055 Jafarzadegan, K., Merwade, V., and Saksena, S.: A geomorphic approach to 100-year floodplain mapping  
1056 for the Conterminous United States, *Journal of Hydrology*, 561, 43-58,  
1057 <https://doi.org/10.1016/j.jhydrol.2018.03.061>, 2018.

1058 Jakubínský, J., Prokopová, M., Raška, P., Salvati, L., Bezak, N., Cudlín, O., Cudlín, P., Purkyt, J., Vezza,  
1059 P., Camporeale, C., Daněk, J., Pástor, M., and Lepeška, T.: Managing floodplains using nature-based  
1060 solutions to support multiple ecosystem functions and services, *WIREs Water*, 8, e1545,  
1061 <https://doi.org/10.1002/wat2.1545>, 2021.

1062 Jin, S., Homer, C., Yang, L., Danielson, P., Dewitz, J., Li, C., Zhu, Z., Xian, G., and Howard, D.: Overall  
1063 Methodology Design for the United States National Land Cover Database 2016 Products, Remote  
1064 Sensing, 11, 2971, 2019.

1065 Jones, C. N., Evenson, G. R., McLaughlin, D. L., Vanderhoof, M. K., Lang, M. W., McCarty, G. W.,  
1066 Golden, H. E., Lane, C. R., and Alexander, L. C.: Estimating restorable wetland water storage at  
1067 landscape scales, Hydrological Processes, 32, 305-313, 10.1002/hyp.11405, 2018.

1068 Karra, K., Kontgis, C., Statman-Weil, Z., Mazzariello, J. C., Mathis, M., & Brumby, S. P. Global land  
1069 use/land cover with Sentinel 2 and deep learning. In: 2021 IEEE International Geoscience and Remote  
1070 Sensing Symposium IGARSS (pp. 4704-4707). IEEE, doi.org/10.1109/IGARSS47720.2021.9553499,  
1071 2021.

1072 Kam, S. P.: Valuing the role of living aquatic resources to rural livelihoods in multiple-use, seasonally-  
1073 inundated wetlands in the Yellow River Basin of China, for improved governance, CGIAR Challenge  
1074 Program on Water & Food, Colombo, Sri Lanka, <https://hdl.handle.net/10568/3859>, 2010.

1075 Kremenetski, K. V., Velichko, A. A., Borisova, O. K., MacDonald, G. M., Smith, L. C., Frey, K. E., and  
1076 Orlova, L. A.: Peatlands of the Western Siberian lowlands: current knowledge on zonation, carbon  
1077 content and Late Quaternary history, Quaternary Science Reviews, 22, 703-723, 2003.

1078 Kundzewicz, Z. W., Hegger, D. L. T., Matczak, P., and Driessen, P. P. J.: Opinion: Flood-risk reduction:  
1079 Structural measures and diverse strategies, Proceedings of the National Academy of Sciences, 115,  
1080 12321-12325, 10.1073/pnas.1818227115, 2018.

1081 Lane, C. R. and D'Amico, E.: Identification of Putative Geographically Isolated Wetlands of the  
1082 Conterminous United States, JAWRA Journal of the American Water Resources Association, 52, 705-  
1083 722, 10.1111/1752-1688.12421, 2016.

1084 Lane, C. R., Leibowitz, S. G., Autrey, B. C., LeDuc, S. D., and Alexander, L. C.: Hydrological, Physical,  
1085 and Chemical Functions and Connectivity of Non-Floodplain Wetlands to Downstream Waters: A  
1086 Review, JAWRA Journal of the American Water Resources Association, 54, 346-371, 10.1111/1752-  
1087 1688.12633, 2018.



1088 Lane, C. R., Creed, I. F., Golden, H. E., Leibowitz, S. G., Mushet, D. M., Rains, M. C., Wu, Q.,  
1089 D'Amico, E., Alexander, L. C., Ali, G. A., Basu, N. B., Bennett, M. G., Christensen, J. R., Cohen, M.  
1090 J., Covino, T. P., DeVries, B., Hill, R. A., Jencso, K., Lang, M. W., McLaughlin, D. L., Rosenberry, D.  
1091 O., Rover, J., and Vanderhoof, M. K.: Vulnerable Waters are Essential to Watershed Resilience,  
1092 Ecosystems, 10.1007/s10021-021-00737-2, 2022.

1093 Lane, C. R., E. D'Amico, J. R. Christensen, H. E. Golden, Q. Wu, and A. Rajib. Global non-floodplain  
1094 wetlands [dataset], [https://gaftp.epa.gov/EPADDataCommons/ORD/Global\\_NonFloodplain\\_Wetlands/](https://gaftp.epa.gov/EPADDataCommons/ORD/Global_NonFloodplain_Wetlands/)  
1095 and <https://doi.org/10.23719/1528331>, 2023.

1096 Lehner, B. and Doll, P.: Development and validation of a global database of lakes, reservoirs and  
1097 wetlands, *Journal of Hydrology*, 296, 1-22, 2004.

1098 Lehner, B. and Grill, G.: Global river hydrography and network routing: baseline data and new  
1099 approaches to study the world's large river systems, *Hydrological Processes*, 27, 2171-2186,  
1100 <https://doi.org/10.1002/hyp.9740>, 2013.

1101 Leibowitz, S.: Geographically Isolated Wetlands: Why We Should Keep the Term, *Wetlands*, 35, 997-  
1102 1003, 10.1007/s13157-015-0691-x, 2015.

1103 Leibowitz, S. G.: Isolated wetlands and their functions: an ecological perspective, *Wetlands*, 22, 517-531,  
1104 2003.

1105 Leibowitz, S. G., Hill, R. A., Creed, I. F., Compton, J. E., Golden, H. E., Weber, M. H., Rains, M. C.,  
1106 Jones, J., C. E., Lee, E. H., Christensen, J. R., Bellmore, R. A., and Lane, C. R.: National hydrologic  
1107 connectivity classification links wetlands with stream water quality, *Nature Water*, 1, 370-380, DOI:  
1108 10.1038/s44221-023-00057-w, 2023.

1109 Liu, D., Cao, C., Chen, W., Ni, X., Tian, R., and Xing, X.: Monitoring and predicting the degradation of a  
1110 semi-arid wetland due to climate change and water abstraction in the Ordos Larus relictus National  
1111 Nature Reserve, China, *Geomatics, Natural Hazards and Risk*, 8, 367-383,  
1112 10.1080/19475705.2016.1220024, 2017.

1113 Makungu, E. and Hughes, D. A.: Understanding and modelling the effects of wetland on the hydrology  
1114 and water resources of large African river basins, *Journal of Hydrology*, 603, 127039,  
1115 <https://doi.org/10.1016/j.jhydrol.2021.127039>, 2021.

1116 Martinis, S., Groth, S., Wieland, M., Knopp, L., and Rättich, M.: Towards a global seasonal and  
1117 permanent reference water product from Sentinel-1/2 data for improved flood mapping, *Remote*  
1118 *Sensing of Environment*, 278, 113077, <https://doi.org/10.1016/j.rse.2022.113077>, 2022.

1119 Marton, J. M., Creed, I. F., Lewis, D., Lane, C. R., Basu, N., Cohen, M. J., and C., C.: Geographically  
1120 isolated wetlands are important biogeochemical reactors on the landscape, *BioScience*, 65, 408-418,  
1121 10.1093/biosci/biv009, 2015.

1122 McCauley, L. A., Anteau, M. J., van der Burg, M. P., and Wiltermuth, M. T.: Land use and wetland  
1123 drainage affect water levels and dynamics of remaining wetlands, *Ecosphere*, 6, art92, 10.1890/ES14-  
1124 00494.1, 2015.

1125 McKenna, O. P., Mushet, D. M., Rosenberry, D. O., and LaBaugh, J. W.: Evidence for a climate-induced  
1126 ecohydrological state shift in wetland ecosystems of the southern Prairie Pothole Region, *Climatic*  
1127 *Change*, 145, 273-287, 10.1007/s10584-017-2097-7, 2017.

1128 McLaughlin, D. L., Kaplan, D. A., and Cohen, M. J.: A significant nexus: Geographically isolated  
1129 wetlands influence landscape hydrology, *Water Resources Research*, 50, 7153-7166,  
1130 10.1002/2013WR015002, 2014.

1131 Merken, R., Deboelpaep, E., Teunen, J., Saura, S., and Koedam, N.: Wetland Suitability and Connectivity  
1132 for Trans-Saharan Migratory Waterbirds, *PLOS ONE*, 10, e0135445, 10.1371/journal.pone.0135445,  
1133 2015.

1134 Messenger, M. L., Lehner, B., Grill, G., Nedeva, I., and Schmitt, O.: Estimating the volume and age of  
1135 water stored in global lakes using a geo-statistical approach, *Nature Communications*, 7, 13603,  
1136 10.1038/ncomms13603, 2016.

1137 Mudashiru, R. B., N. Sabtu, I. Abustan and W. Balogun. Flood hazard mapping methods: A review.  
1138 Journal of Hydrology, 603, 126846, 2021.

1139 Mushet, D., Calhoun, A., Alexander, L., Cohen, M., DeKeyser, E., Fowler, L., Lane, C., Lang, M., Rains,  
1140 M., and Walls, S.: Geographically Isolated Wetlands: Rethinking a Misnomer, Wetlands, 35, 423-431,  
1141 10.1007/s13157-015-0631-9, 2015.

1142 Mushet, D. M., Alexander, L. C., Bennett, M., Schofield, K., Christensen, J. R., Ali, G., Pollard, A., Fritz,  
1143 K., and Lang, M. W.: Differing Modes of Biotic Connectivity within Freshwater Ecosystem Mosaics,  
1144 JAWRA Journal of the American Water Resources Association, 55, 307-317, 10.1111/1752-  
1145 1688.12683, 2019.

1146 Nardi, F., Annis, A., Di Baldassarre, G., Vivoni, E. R., and Grimaldi, S.: GFPLAIN250m, a global high-  
1147 resolution dataset of Earth's floodplains, Scientific Data, 6, 180309, 10.1038/sdata.2018.309, 2019.

1148 National Landcover Database (NLCD) 2019 NLCD Land Cover (CONUS), <https://www.mrlc.gov/data>,  
1149 last accessed 22 December 2022.

1150 Nitzsche, K. N., Kalettka, T., Premke, K., Lischeid, G., Gessler, A., and Kayler, Z. E.: Land-use and  
1151 hydroperiod affect kettle hole sediment carbon and nitrogen biogeochemistry, Science of The Total  
1152 Environment, 574, 46-56, <http://dx.doi.org/10.1016/j.scitotenv.2016.09.003>, 2017.

1153 Olefeldt, D., Hovemyr, M., Kuhn, M. A., Bastviken, D., Bohn, T. J., Connolly, J., Crill, P., Euskirchen, E.  
1154 S., Finkelstein, S. A., Genet, H., Grosse, G., Harris, L. I., Heffernan, L., Helbig, M., Hugelius, G.,  
1155 Hutchins, R., Juutinen, S., Lara, M. J., Malhotra, A., Manies, K., McGuire, A. D., Natali, S. M.,  
1156 O'Donnell, J. A., Parmentier, F. J. W., Räsänen, A., Schädel, C., Sonnentag, O., Strack, M., Tank, S. E.,  
1157 Treat, C., Varner, R. K., Virtanen, T., Warren, R. K., and Watts, J. D.: The Boreal–Arctic Wetland and  
1158 Lake Dataset (BAWLD), Earth Syst. Sci. Data, 13, 5127-5149, 10.5194/essd-13-5127-2021, 2021.

1159 Pappenberger, F., E. Dutra, F. Wetterhall and H. L. Cloke. Deriving global flood hazard maps of fluvial  
1160 floods through a physical model cascade. Hydrol. Earth Syst. Sci., 16, 11, 4143-4156, 2012.

1161 Pekel, J.-F., Cottam, A., Gorelick, N., and Belward, A. S.: High-resolution mapping of global surface  
1162 water and its long-term changes, *Nature*, 540, 418-422, 10.1038/nature20584, 2016.

1163 Prigent, C., Papa, F., Aires, F., Rossow, W. B., and Matthews, E.: Global inundation dynamics inferred  
1164 from multiple satellite observations, 1993–2000, *Journal of Geophysical Research: Atmospheres*, 112,  
1165 <https://doi.org/10.1029/2006JD007847>, 2007.

1166 PRISM Climate Group, Parameter-elevation Regressions on Independent Slopes Model,  
1167 [prism.oregonstate.edu/](http://prism.oregonstate.edu/), last accessed 22 December 2022.

1168 Rains, M. C., Leibowitz, S. G., Cohen, M. J., Creed, I. F., Golden, H. E., Jawitz, J. W., Kalla, P., Lane, C.  
1169 R., Lang, M. W., and McLaughlin, D. L.: Geographically isolated wetlands are part of the hydrological  
1170 landscape, *Hydrological Processes*, 30, 153-160, 10.1002/hyp.10610, 2016.

1171 Rajib, A., Golden, H. E., Lane, C. R., and Wu, Q.: Surface depression and wetland water storage  
1172 improves major river basin hydrologic predictions, *Water Resources Research*, 56, e2019WR026561,  
1173 <https://doi.org/10.1029/2019WR026561>, 2020.

1174 Rajib, A., Zheng, Q., Golden, H. E., Wu, Q., Lane, C. R., Christensen, J. R., Morrison, R. R., Annis, A.,  
1175 and Nardi, F.: The changing face of floodplains in the Mississippi River Basin detected by a 60-year  
1176 land use change dataset, *Scientific Data*, 8, 271, 10.1038/s41597-021-01048-w, 2021.

1177 Robarts, R., Zhulidov, A., and Pavlov, D.: The State of knowledge about wetlands and their future under  
1178 aspects of global climate change: the situation in Russia, *Aquatic Sciences*, 75, 27-38, 10.1007/s00027-  
1179 011-0230-7, 2013.

1180 Rodrigues, L. N., Sano, E. E., Steenhuis, T. S., and Passo, D. P.: Estimation of Small Reservoir Storage  
1181 Capacities with Remote Sensing in the Brazilian Savannah Region, *Water Resources Management*, 26,  
1182 873-882, 10.1007/s11269-011-9941-8, 2012.

1183 Rodríguez-Rodríguez, M., Aguilera, H., Guardiola-Albert, C., and Fernández-Ayuso, A.: Climate  
1184 Influence Vs. Local Drivers in Surface Water-Groundwater Interactions in Eight Ponds of Doñana  
1185 National Park (Southern Spain), *Wetlands*, 41, 25, 10.1007/s13157-021-01425-6, 2021.

1186 Rudari, R., Silvestro, F., Campo, L., Rebori, N., Boni, G., and Herold, C. Improvement of the global  
1187 flood model for the GAR 2015. United Nations Office for Disaster Risk Reduction (UNISDR), Centro  
1188 Internazionale in Monitoraggio Ambientale (CIMA), UNEP GRID-Arendal (GRID-Arendal): Geneva,  
1189 Switzerland, 69, 2015.

1190 Sampson, C. C., Smith, A. M., Bates, P. D., Neal, J. C., Alfieri, L., and Freer, J. E.: A high-resolution  
1191 global flood hazard model, *Water Resources Research*, 51, 7358-7381, 10.1002/2015WR016954, 2015.

1192 Samways, M. J., Deacon, C., Kietzka, G. J., Pryke, J. S., Vorster, C., and Simaika, J. P.: Value of  
1193 artificial ponds for aquatic insects in drought-prone southern Africa: a review, *Biodiversity and  
1194 Conservation*, 29, 3131-3150, 10.1007/s10531-020-02020-7, 2020.

1195 Sangwan, N. and Merwade, V.: A Faster and Economical Approach to Floodplain Mapping Using Soil  
1196 Information, *JAWRA Journal of the American Water Resources Association*, 51, 1286-1304,  
1197 10.1111/1752-1688.12306, 2015.

1198 Schofield, K. A., Alexander, L. C., Ridley, C. E., Vanderhoof, M. K., Fritz, K. M., Autrey, B. C.,  
1199 DeMeester, J. E., Kepner, W. G., Lane, C. R., Leibowitz, S. G., and Pollard, A. I.: Biota Connect  
1200 Aquatic Habitats throughout Freshwater Ecosystem Mosaics, *JAWRA Journal of the American Water  
1201 Resources Association*, 54, 372-399, 10.1111/1752-1688.12634, 2018.

1202 Serran, J. N., Creed, I. F., Ameli, A. A., and Aldred, D. A.: Estimating rates of wetland loss using power-  
1203 law functions, *Wetlands*, 38, 109-120, 10.1007/s13157-017-0960-y, 2017.

1204 Shaw, D. A., Vanderkamp, G., Conly, F. M., Pietroniro, A., and Martz, L.: The Fill–Spill Hydrology of  
1205 Prairie Wetland Complexes during Drought and Deluge, *Hydrological Processes*, 26, 3147-3156,  
1206 10.1002/hyp.8390, 2012.

1207 Smith, L. L., Subalusky, A. L., Atkinson, C. L., Earl, J. E., Mushet, D. M., Scott, D. E., Lance, S. L., and  
1208 Johnson, S. A.: Biological Connectivity of Seasonally Poned Wetlands across Spatial and Temporal  
1209 Scales, *JAWRA Journal of the American Water Resources Association*, 55, 334-353, 10.1111/1752-  
1210 1688.12682, 2019.

1211 Strahler, A. N.: Quantitative analysis of watershed geomorphology, American Geophysical Union  
1212 Transactions, 38, 913-920, 1957.

1213 Sullivan, S. M. P., Rains, M. C., and Rodewald, A. D.: Opinion: The proposed change to the definition of  
1214 “waters of the United States” flouts sound science, Proceedings of the National Academy of Sciences,  
1215 116, 11558, 10.1073/pnas.1907489116, 2019.

1216 Tayefi, V., Lane, S. N., Hardy, R. J., and Yu, D.: A comparison of one- and two-dimensional approaches  
1217 to modelling flood inundation over complex upland floodplains, Hydrological Processes, 21, 3190-  
1218 3202, 10.1002/hyp.6523, 2007.

1219 Tootchi, A., Jost, A., and Ducharme, A.: Multi-source global wetland maps combining surface water  
1220 imagery and groundwater constraints, Earth Syst. Sci. Data, 11, 189-220, 10.5194/essd-11-189-2019,  
1221 2019.

1222 Tsendbazar, N., Herold, M., Li, L., Tarko, A., de Bruin, S., Masiliunas, D., Lesiv, M., Fritz, S., Buchhorn,  
1223 M., Smets, B., Van De Kerchove, R., and Duerauer, M.: Towards operational validation of annual  
1224 global land cover maps, Remote Sensing of Environment, 266, 112686,  
1225 <https://doi.org/10.1016/j.rse.2021.112686>, 2021.

1226 Tullos, D.: Opinion: How to achieve better flood-risk governance in the United States, Proceedings of the  
1227 National Academy of Sciences, 115, 3731-3734, 10.1073/pnas.1722412115, 2018.

1228 Uden, D. R., Allen, C. R., Bishop, A. A., Grosse, R., Jorgensen, C. F., LaGrange, T. G., Stutheit, R. G.,  
1229 and Vrtiska, M. P.: Predictions of future ephemeral springtime waterbird stopover habitat availability  
1230 under global change, Ecosphere, 6, 1-26, 10.1890/ES15-00256.1, 2015.

1231 United States Geological Survey (USGS) National Elevation Dataset, [https://www.usgs.gov/3d-elevation-](https://www.usgs.gov/3d-elevation-program)  
1232 program, last accessed 22 December 2022.

1233 United States Geological Survey (USGS) Watershed Boundary Dataset, [https://www.usgs.gov/national-](https://www.usgs.gov/national-hydrography/access-national-hydrography-products)  
1234 hydrography/access-national-hydrography-products, last accessed 22 December 2022.

1235 Van Meter, K. J. and Basu, N. B.: Signatures of human impact: size distributions and spatial organization  
1236 of wetlands in the Prairie Pothole landscape, *Ecological Applications*, 25, 451-465, 10.1890/14-0662.1,  
1237 2015.

1238 Van Meter, K. J., Basu, N. B., Tate, E., and Wyckoff, J.: Monsoon Harvests: The Living Legacies of  
1239 Rainwater Harvesting Systems in South India, *Environmental Science & Technology*, 48, 4217-4225,  
1240 10.1021/es4040182, 2014.

1241 Vanderhoof, M. K. and Lane, C. R.: The potential role of very high-resolution imagery to characterise  
1242 lake, wetland and stream systems across the Prairie Pothole Region, United States, *International Journal*  
1243 *of Remote Sensing*, 40, 5768-5798, 10.1080/01431161.2019.1582112, 2019.

1244 Wania, R., Melton, J. R., Hodson, E. L., Poulter, B., Ringeval, B., Spahni, R., Bohn, T., Avis, C. A.,  
1245 Chen, G., Eliseev, A. V., Hopcroft, P. O., Riley, W. J., Subin, Z. M., Tian, H., van Bodegom, P. M.,  
1246 Kleinen, T., Yu, Z. C., Singarayer, J. S., Zürcher, S., Lettenmaier, D. P., Beerling, D. J., Denisov, S. N.,  
1247 Prigent, C., Papa, F., and Kaplan, J. O.: Present state of global wetland extent and wetland methane  
1248 modelling: methodology of a model inter-comparison project (WETCHIMP), *Geosci. Model Dev.*, 6,  
1249 617-641, 10.5194/gmd-6-617-2013, 2013.

1250 Werner, M. G. F., Hunter, N. M., and Bates, P. D.: Identifiability of distributed floodplain roughness  
1251 values in flood extent estimation, *Journal of Hydrology*, 314, 139-157,  
1252 <https://doi.org/10.1016/j.jhydrol.2005.03.012>, 2005.

1253 Wickham, J., Stehman, S. V., Sorenson, D. G., Gass, L., and Dewitz, J. A.: Thematic accuracy assessment  
1254 of the NLCD 2016 land cover for the conterminous United States, *Remote Sensing of Environment*,  
1255 257, 112357, <https://doi.org/10.1016/j.rse.2021.112357>, 2021.

1256 Wing, O. E. J., Bates, P. D., Sampson, C. C., Smith, A. M., Johnson, K. A., and Erickson, T. A.:  
1257 Validation of a 30 m resolution flood hazard model of the conterminous United States, *Water Resources*  
1258 *Research*, 53, 7968-7986, 10.1002/2017WR020917, 2017.

1259 Winsemius, H. C., L. P. H. Van Beek, B. Jongman, P. J. Ward and A. Bouwman. A framework for global  
1260 river flood risk assessments, *Hydrol. Earth Syst. Sci.*, 17, 5, 1871-1892, 2013.

1261 Winter, T. C.: The Vulnerability of Wetlands to Climate Change: A Hydrologic Landscape Perspective,  
1262 JAWRA Journal of the American Water Resources Association, 36, 305-311, 10.1111/j.1752-  
1263 1688.2000.tb04269.x, 2000.

1264 Winter, T. C., J.W. Harvey, O.L. Franke, and Alley, W. M.: Ground Water and Surface Water: A Single  
1265 Resoure, U.S. Government Printing Office, Washington, DC., 1998.

1266 Woznicki, S. A., Baynes, J., Panlasigui, S., Mehaffey, M., and Neale, A.: Development of a spatially  
1267 complete floodplain map of the conterminous United States using random forest, Science of The Total  
1268 Environment, 647, 942-953, <https://doi.org/10.1016/j.scitotenv.2018.07.353>, 2019.

1269 Wu, Q., Lane, C. R., Wang, L., Vanderhoof, M. K., Christensen, J. R., and Liu, H.: Efficient Delineation  
1270 of Nested Depression Hierarchy in Digital Elevation Models for Hydrological Analysis Using Level-Set  
1271 Method, JAWRA Journal of the American Water Resources Association, 55, 354-368, 10.1111/1752-  
1272 1688.12689, 2019a.

1273 Wu, Q., Lane, C. R., Li, X., Zhao, K., Zhou, Y., Clinton, N., DeVries, B., Golden, H. E., and Lang, M.  
1274 W.: Integrating LiDAR data and multi-temporal aerial imagery to map wetland inundation dynamics  
1275 using Google Earth Engine, Remote Sensing of Environment, 228, 1-13,  
1276 <https://doi.org/10.1016/j.rse.2019.04.015>, 2019b.

1277 Xi, Y., Peng, S., Ducharne, A., Ciais, P., Gumbricht, T., Jimenez, C., Poulter, B., Prigent, C., Qiu, C.,  
1278 Saunois, M., and Zhang, Z.: Gridded maps of wetlands dynamics over mid-low latitudes for 1980–2020  
1279 based on TOPMODEL, Scientific Data, 9, 347, 10.1038/s41597-022-01460-w, 2022.

1280 Yamazaki, D., S. Kanae, H. Kim and T. Oki. A physically based description of floodplain inundation  
1281 dynamics in a global river routing model, Water Resources Research, 47, 4, 2011.

1282 Yamazaki, D., Ikeshima, D., Sosa, J., Bates, P. D., Allen, G., and Pavelsky, T.: MERIT Hydro: A high-  
1283 resolution global hydrography map based on latest topography datasets, Water Resources Research, 55,  
1284 5053-5073, 10.1029/2019wr024873, 2019.

1285 Zanaga, D., Van De Kerchove, R., De Keersmaecker, W., Souverijns, N., Brockmann, C., Quast, R.,  
1286 Wevers, J., Grosu, A., Paccini, A., Vergnaud, S., Cartus, O., Santoro, M., Fritz, S., Georgieva, I., Lesiv,



1287 M., Carter, S., Herold, M., Li, Linlin, Tsendbazar, N.E., Ramoïno, F., Arino, O.: ESA WorldCover 10  
1288 m 2020 v100, <https://doi.org/10.5281/zenodo.5571936> 2021.

1289 Zedler, J. B. and Kercher, S.: Causes and consequences of invasive plants in wetlands: Opportunities,  
1290 opportunists, and outcomes, *Critical Reviews in Plant Sciences*, 23, 431-452, 2004.

1291 Zhang, X., L. Liu, T. Zhao, X. Chen, S. Lin, J. Wang, J. Mi and W. Liu. GWL\_FCS30: global 30 m  
1292 wetland map with fine classification system using multi-sourced and time-series remote sensing  
1293 imagery in 2020. *Earth Syst. Sci. Data* 15, 265-293, 2023.

1294 Zhu, Y., Xu, Y., Deng, X., Kwon, H., and Qin, Z.: Peatland Loss in Southeast Asia Contributing to U.S.  
1295 Biofuel's Greenhouse Gas Emissions, *Environmental Science & Technology*, 10.1021/acs.est.2c01561,  
1296 2022.

1297